

Learning Heuristics for Transit Network Design and Improvement with Deep Reinforcement Learning

Andrew Holliday · Ahmed El-Geneidy · Gregory Dudek

the date of receipt and acceptance should be inserted later

Abstract Transit agencies world-wide face tightening budgets. To maintain quality of service while cutting costs, efficient transit network design is essential. But planning a network of public transit routes is a challenging optimization problem. The most successful approaches to date use metaheuristic algorithms to search through the space of solutions by applying low-level heuristics that randomly alter routes in a network. The design of these low-level heuristics has a major impact on the quality of the result. In this paper we use deep reinforcement learning with graph neural nets to learn low-level heuristics for an evolutionary algorithm, instead of designing them manually. These learned heuristics improve the algorithm's results on benchmark synthetic cities with 70 nodes or more, and obtain state-of-the-art results when optimizing operating costs. They also improve upon a simulation of the real transit network in the city of Laval, Canada, by as much as 54% and 18% on two key metrics, and offer cost savings of up to 12% over the city's existing transit network.

Acknowledgements

We thank the Société de Transport de Laval for the map data and transportation data they provided, and the Agence Métropolitaine de Transport for the origin-destination dataset they provided. This data was essential to the experiments presented in this paper. We also gratefully acknowledge the funding they received from NSERC in support of this work. And we thank Joshua Katz, the room-mate of the first author, for acting as a sounding board for ideas and giving feedback on our experimental designs.

Address(es) of author(s) should be given

1 INTRODUCTION

The COVID-19 pandemic resulted in declines in transit ridership in cities worldwide (Liu et al., 2020). This has led to a financial crisis for municipal transit agencies, putting them under pressure to reduce transit operating costs (Kar et al., 2022). But if cost-cutting leads to reduced quality of service, ridership may be harmed further, leading to a downward spiral of service quality and income. Agencies find themselves having to do more with less. Thus, the layout of transit networks is key, as a well-planned layout can cut operating costs and improve service quality, making every dollar count. But updating a transit network is not to be undertaken lightly. For rail transit, changing a network's layout requires infrastructural changes that may be prohibitively costly. And even for bus transit, network redesigns can be costly and disruptive for users and bus drivers. So it is vital to agencies that they get design right the first time. Good algorithms for the Transit Network Design Problem (NDP) can therefore be very useful to transit agencies.

The NDP is the problem of designing a set of transit routes for a city that satisfy one or more objectives, such as meeting all travel demand and minimizing operating costs. It is an NP-complete problem that has commonalities with the travelling salesman problem (TSP) and vehicle routing problem (VRP), but is more complex than these famously-challenging problems. Furthermore, real-world cities may have hundreds or even thousands of possible stop locations. So analytical optimization approaches are infeasible. For this reason, the most successful algorithms to-date have been metaheuristic algorithms. These work by repeatedly applying one or more low-level heuristics that randomly modify a solution, and guiding this random search to-

wards more promising solutions over many iterations by means of a metaheuristic such as natural selection (as in evolutionary algorithms) or metallic annealing (as in simulated annealing). Many different metaheuristics for guiding the search have been proposed, as have a range of low-level heuristics for transit network design. While these algorithms can find good solutions in many cases, real-world transit networks are still commonly designed by hand (Durán-Micco and Vansteenwegen, 2022).

The low-level heuristics used in these metaheuristic algorithms randomly alter the solutions under consideration, with different heuristics making different kinds of alterations: one heuristic may randomly select a stop on an existing route and remove it from the route, while another may randomly add a stop at one end of a route, and another may select two stops on a route at random and exchange them. What most low-level heuristics have in common is that they are uniformly random: no aspect of the particular scenario affects the heuristic’s likelihood of selecting one action versus another. We here wish to consider whether a machine learning system could act as a more intelligent heuristic, by learning to use information about the city and the current transit network to select the most promising alterations.

In our prior work (Holliday and Dudek, 2023), we trained a neural net to plan a transit network from scratch, and showed that using this transit network as the initial solution improved the solutions found by two metaheuristic algorithms. That policy assembles a transit route by concatenating shortest paths in the city’s street network that share end points, using the neural net to select the next shortest path to be included at each step. By repeating this process for each route that is needed, it assembles a complete transit network.

Our subsequent work (Holliday and Dudek, 2024) built on this by considering whether the graph neural net (GNN) policy can benefit a metaheuristic algorithm by serving as a learned low-level heuristic. To test this, we implemented the evolutionary algorithm of Nikolić and Teodorović (2013). We compared it with a variant in which we replaced one of its low-level heuristics with a heuristic that applies the GNN policy to plan one new route. The GNN policy was first trained in a similar manner as in Holliday and Dudek (2023), before being applied in the evolutionary algorithm. We found that this learned heuristic considerably improves the algorithm’s performance on cities with 70 nodes or more.

In the present work, we expand on these results in several ways. We present new benchmark results using an improved GNN model and an improved evolutionary algorithm. We also perform ablation studies to analyze

the importance of different components of our neural-evolutionary algorithm hybrid. As part of these ablations, we consider a novel unlearned low-level heuristic, where shortest paths with common endpoints are joined uniformly at random instead of according to the GNN policy. Interestingly, we find that in the narrow case where we are only concerned with minimizing passenger travel time, this heuristic outperforms both the baseline heuristics of Nikolić and Teodorović (2013) and our GNN heuristic; in most other cases, however, our GNN heuristic performs better.

We compare the performance of our learned and unlearned heuristics with other results on the widely-used Mandl (Mandl, 1980) and Mumford (Mumford, 2013a) benchmark cities. We find that the unlearned heuristic obtains results comparable to the state of the art when minimizing only the passengers’ travel time, while the GNN heuristic outperforms the previous state of the art when minimizing only the cost to operators by as much as 13%.

Finally, we go beyond our earlier work by applying our heuristics to real data from the city of Laval, Canada, a very large real-world problem instance. We show that our learned heuristic can be used to plan transit networks for Laval that, in simulation, exceed the performance of the city’s existing transit system by a wide margin, for three distinct optimization goals. These results show that our heuristics may allow transit agencies to offer better service at less cost.

2 BACKGROUND AND RELATED WORK

2.1 Neural Nets for Optimization Problems

As documented by Bengio et al. (2021), there has recently been growing interest in the application of machine learning techniques to combinatorial optimization (CO) problems such as the TSP.

Vinyals et al. (2015) proposed a neural net model called a Pointer Network, and trained it via supervised learning to solve TSP instances. Subsequent work, such as that of Dai et al. (2017), Kool et al. (2019), and Sykora et al. (2020), has built on this. These works use similar neural net models, in combination with reinforcement learning algorithms, to train neural nets to construct CO solutions. These have attained impressive performance on the TSP, the VRP, and other CO problems. Choo et al. (2022) present a hybrid algorithm of Monte Carlo Tree Search and Beam Search that draws better sample solutions for the TSP and Capacitated VRP (CVRP) from a neural net policy like that of Kool et al. (2019). Mundhenk et al. (2021) trains a recurrent neural net (RNN) via reinforcement learning (RL)

to construct a starting population of solutions to a genetic algorithm, the outputs of which are used to further train the RNN. Fu et al. (2021) train a model on small TSP instances and present an algorithm that applies the model to much larger instances.

These approaches all belong to the family of “construction” methods, which solve a CO problem by starting with an “empty” solution and adding to it in steps, ending once the solution is complete - for example, when all nodes have been visited in the TSP. The solutions from these neural construction methods come close to the quality of those from specialized TSP algorithms such as Concorde (Applegate et al., 2001), while requiring much less run-time to compute (Kool et al., 2019).

By contrast with construction methods, “Improvement” methods start with a complete solution and repeatedly modify it, searching through the solution space for improvements. These are generally more computationally costly than construction methods but can yield better solutions to CO problems. Evolutionary algorithms belong to this category. Some work has considered training neural nets to choose the search moves to be made at each step of an improvement method (Hottung and Tierney, 2019; Chen and Tian, 2019; d O Costa et al., 2020; Wu et al., 2021; Ma et al., 2021), and Kim et al. (2021) train one neural net to construct a set of initial solutions, and another to modify and improve them. This work has shown impressive performance on the TSP and other CO problems. Our work belongs to this family, in that we train a neural net to solve instances of the transit network design problem, and then use it to modify solutions within an improvement method.

In most of the above work, the neural net models used are Graph neural nets (GNNs), a type of neural net model that is designed to operate on graph-structured data (Bruna et al., 2013; Kipf and Welling, 2016; Defferrard et al., 2016; Duvenaud et al., 2015). These have been applied in many other domains, including the analysis of large web graphs (Ying et al., 2018), the design of printed circuit boards (Mirhoseini et al., 2021), and the prediction of chemical properties of molecules (Duvenaud et al., 2015; Gilmer et al., 2017). An overview of GNNs is provided by Battaglia et al. (2018). Like many CO problems, the transit network design problem lends itself to being described as a graph problem, so we use GNN models here as well.

In most CO problems, it is difficult to find globally optimal solutions but easier gauge the quality of a given solution. As Bengio et al. (2021) note, this makes reinforcement learning, in which machine learning systems are trained to maximize a measure of reward, a natural

fit to CO problems. Most of the work cited in this section uses RL methods to train neural net models. We do the same here, applying a method similar to that of Kool et al. (2019) to the NDP.

2.2 Optimization of Public Transit

The NDP is an NP-complete problem (Quak, 2003), meaning that it is impractical to find optimal solutions for most cases. While analytical optimization and mathematical programming methods have been successful on small instances (van Nes, 2003; Guan et al., 2006), they struggle to realistically represent the problem (Guihaire and Hao, 2008; Kepaptsoglou and Karlaftis, 2009). Metaheuristic approaches, as defined by Sörensen et al. (2018), have thus been more widely applied.

The most widely-used metaheuristics for the NDP have been genetic algorithms, simulated annealing, and ant-colony optimization, along with hybrids of these methods (Guihaire and Hao, 2008; Kepaptsoglou and Karlaftis, 2009; Durán-Micco and Vansteenwegen, 2022; Yang and Jiang, 2020; Hüßelmann et al., 2023), achieving impressive results. Recent work has also shown other metaheuristics can be used with success, such as sequence-based selection hyper-heuristics (Ahmed et al., 2019), beam search (Islam et al., 2019), and particle swarms (Lin and Tang, 2022). Many different low-level heuristics have been applied within these metaheuristic algorithms, but most have in common that they select among possible neighbourhood moves uniformly at random.

One exception is Hüßelmann et al. (2023). For two heuristics, the authors design a simple model of how each modification the heuristic could make would affect solution quality. They use this model to give the different modifications different probabilities of being selected. The resulting heuristics obtain state-of-the-art results. However, their simple model ignores both actions’ effect on passenger trips involving transfers, and the impact of the users’ preference over different parts of the cost function. By contrast, the method we propose **learns** a model of actions’ impact to assign probabilities to them, and does so based on a richer set of inputs.

While neural nets have often been used for predictive problems in urban mobility (Xiong and Schneider, 1992; Rodrigue, 1997; Chien et al., 2002; Jeong and Rilett, 2004; Çodur and Tortum, 2009; Li et al., 2020) and for other transit optimization problems such as scheduling, passenger flow control, and traffic signal control (Zou et al., 2006; Ai et al., 2022; Yan et al., 2023; Jiang et al., 2018; Wang et al., 2024), they have not often been applied to the NDP, and neither has

RL. Two recent examples are Darwish et al. (2020) and Yoo et al. (2023). Both use RL to design routes and a schedule for the Mandl benchmark (Mandl, 1980), a single small city with just 15 transit stops, and both obtain good results. Darwish et al. (2020) use a GNN approach inspired by Kool et al. (2019); in our own work we experimented with a nearly identical approach to Darwish et al. (2020), but found it did not scale beyond very small instances. Meanwhile, Yoo et al. (2023) uses tabular RL, a type of approach which is known to scale poorly to large sizes of problem. Both of these approaches also require a new model to be trained on each problem instance. Our approach, by contrast, is able to find good solutions for realistically-sized NDP instances of more than 600 nodes, and can be applied to problem instances unseen during model training.

In our prior work (Holliday and Dudek, 2023), we trained a GNN to construct a transit network one route at a time, and used the GNN to provide initial solutions to two NDP improvement algorithms: the evolutionary algorithm of Nikolić and Teodorović (2013) and the hyperheuristic algorithm of Ahmed et al. (2019). We found that this improved the quality of the solutions found by both methods. In the present work, we consider a similar GNN architecture and training procedure, but we use it as one of the low-level heuristics that is applied at each step of the improvement algorithm.

3 TRANSIT NETWORK DESIGN PROBLEM

In the Transit Network Design Problem, one is given an augmented graph that represents a city:

$$\mathcal{C} = (\mathcal{N}, \mathcal{E}_s, D) \quad (1)$$

This is comprised of a set \mathcal{N} of n nodes, representing candidate stop locations; a set \mathcal{E}_s of street edges (i, j, τ_{ij}) connecting the nodes, with weights τ_{ij} indicating drive times on those streets; and an $n \times n$ Origin-Destination (OD) matrix D giving the travel demand (in number of trips) between every pair of nodes in \mathcal{N} . The goal is to propose a transit network, which is a set of routes \mathcal{R} that minimize a cost function $C : \mathcal{C}, \mathcal{R} \rightarrow \mathbb{R}^+$, where each route r is a sequence of nodes in \mathcal{N} . The transit network \mathcal{R} is subject to the following constraints:

1. \mathcal{R} must be connected, providing some path over transit between every pair of nodes $(i, j) \in \mathcal{N}$ for which $D_{ij} > 0$.
2. \mathcal{R} must contain exactly S routes ($|\mathcal{R}| = S$), where S is a parameter set by the user.

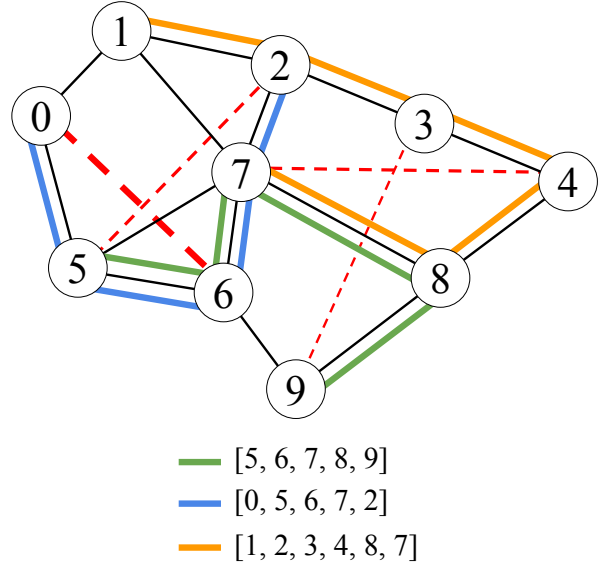


Fig. 1: An example city graph with ten numbered nodes and three routes. Street edges are black, routes are in colour, and two example demands are shown by dashed red lines. The edges of the three routes form a subgraph of the street graph $(\mathcal{N}, \mathcal{E}_s)$. All nodes are connected by this subgraph, so the three routes form a valid transit network. The demand between nodes 2 and 5 and between 0 and 6 can be satisfied directly by riding on the blue line, and the demand from 7 to 4 by the orange line. Meanwhile, the demand from 3 to 9 requires one transfer: passengers must ride the orange line from node 3 to 8, and then the green line from node 8 to 9.

3. Every route $r \in \mathcal{R}$ must obey the limit on number of stops per route: $MIN \leq |r| \leq MAX$, where MIN and MAX are parameters set by the user.
4. A route $r \in \mathcal{R}$ may not contain cycles; each node $i \in \mathcal{N}$ can appear in r at most once.

We here deal with the symmetric NDP, that is: $D = D^\top$, $(i, j, \tau_{ij}) \in \mathcal{E}_s$ iff. $(j, i, \tau_{ij}) \in \mathcal{E}_s$, and all routes are traversed both forwards and backwards by vehicles on them. An example city graph with a transit network is shown in Figure 1.

3.1 Markov Decision Process Formulation

A Markov Decision Process (MDP) is a formalism commonly used to define problems in RL (Sutton and Barto, 2018, Chapter 3). In an MDP, an **agent** interacts with an environment over a series of timesteps. At each timestep t , the environment is in a **state** $s_t \in \mathcal{S}$, and the agent takes some **action** $a_t \in \mathcal{A}_t$, where \mathcal{A}_t is the set of available actions at t . The environment

then transitions to a new state $s_{t+1} \in \mathcal{S}$ according to the state transition distribution $P(s_{t+1}|s_t, a_t)$, and the agent receives a numerical **reward** $R_t \in \mathbb{R}$ according to the reward distribution $P(R_t|s_t, a_t, s_{t+1})$. The agent chooses actions according to its **policy** $\pi(a_t|s_t)$, which is a probability distribution over \mathcal{A}_t given s_t in each state. In RL, the goal is to learn a policy π that maximizes the return G_t , defined as a time-discounted sum of rewards:

$$G_t = \sum_{t'=t}^{t_{end}} \gamma^{t'-t} R_{t'} \quad (2)$$

Where $\gamma \in [0, 1]$ is a parameter that discounts rewards farther in the future, and t_{end} is the final timestep of the MDP. The sequence of states visited, actions taken, and rewards received from $t = 0$ to $t = t_{end}$ constitutes one **episode**.

We here describe the MDP we use to represent a construction approach to the Transit Network Design Problem. As shown in Equation 3, the state s_t is composed of the set of routes \mathcal{R}_t planned so far, and an incomplete route r_t which is being planned.

$$s_t = (\mathcal{R}_t, r_t) \quad (3)$$

The starting state is $s_0 = (\mathcal{R}_0 = \{\}, r_0 = [])$. At a high level, the MDP alternates at every timestep between two modes: on odd-numbered timesteps, the agent selects an extension to the route r_t that it is currently planning; on even-numbered timesteps, the agent chooses whether to stop extending r_t and add it to \mathcal{R}_t .

On odd-numbered timesteps, the available actions are drawn from SP, the set of shortest paths between all node pairs. If $r_t = []$, then $\mathcal{A}_t = \{a \mid a \in \text{SP}, |a| \leq \text{MAX}\}$. Otherwise, \mathcal{A}_t is comprised of paths $a \in \text{SP}$ satisfying all of the following conditions:

- $(i, j, \tau_{ij}) \in \mathcal{E}_s$, where i is the first node of a and j is the last node of r_t , or vice-versa
- a and r_t have no nodes in common
- $|a| \leq \text{MAX} - |r_t|$

Once a path $a_t \in \mathcal{A}_t$ is chosen, r_{t+1} is formed by appending a_t to the beginning or end of r_t as appropriate: $r_{t+1} = \text{combine}(r_t, a_t)$.

On even-numbered timesteps, the action space depends on the number of stops in r_t :

$$\mathcal{A}_t = \begin{cases} \{\text{continue}\} & \text{if } |r_t| < \text{MIN} \\ \{\text{halt}\} & \text{if } |r_t| = \text{MAX} \\ \{\text{continue}, \text{halt}\} & \text{otherwise} \end{cases} \quad (4)$$

If $a_t = \text{halt}$, r_t is added to \mathcal{R}_t to get \mathcal{R}_{t+1} , and $r_{t+1} = []$ is a new empty route. If $a_t = \text{continue}$, then \mathcal{R}_{t+1} and r_{t+1} are unchanged from timestep t .

When $|\mathcal{R}_t| = S$, the episode terminates, giving the final reward $R_t = -C(\mathcal{C}, \mathcal{R}_t)$. At all prior steps, $R_t = 0$.

This MDP formalization imposes some helpful biases on the solution space. First, it requires any route connecting i and j to stop at all nodes along some path between i and j , biasing planned routes towards covering more nodes. Second, it biases routes towards directness by forcing them to be composed of shortest paths. While policy may construct arbitrarily indirect routes by choosing paths with length 2 at every step, this is unlikely because in a realistic street graph, the majority of paths in SP are longer than one edge. Third, the alternation between deciding to continue or halt a route and deciding how to extend the route means that the probability of halting does not depend on how many different extensions are available.

3.2 Cost Function

Our NDP cost function has three components. The cost to passengers, C_p , is the average passenger trip time over the network:

$$C_p(\mathcal{C}, \mathcal{R}) = \frac{\sum_{i,j} D_{ij} \tau_{\mathcal{R}ij}}{\sum_{i,j} D_{ij}} \quad (5)$$

Where $\tau_{\mathcal{R}ij}$ is the time of the shortest transit trip from i to j given \mathcal{R} , including a time penalty p_T for each transfer.

The operating cost is the total driving time of the routes, or total route time:

$$C_o(\mathcal{C}, \mathcal{R}) = \sum_{r \in \mathcal{R}} \tau_r \quad (6)$$

Where τ_r is the time needed to completely traverse a route r in one direction.

To enforce the constraints on \mathcal{R} , we use a third term C_c , which is the fraction of node pairs that are not connected by \mathcal{R} plus a measure of how much $|r| > \text{MAX}$ or $|r| < \text{MIN}$ across all routes. The cost function is then:

$$C(\mathcal{C}, \mathcal{R}) = \alpha w_p C_p + (1 - \alpha) w_o C_o + \beta C_c \quad (7)$$

The weight $\alpha \in [0, 1]$ controls the trade-off between passenger and operating costs, while β is the penalty assigned for each cost violation. w_p and w_o are re-scaling constants chosen so that $w_p C_p$ and $w_o C_o$ both vary roughly over the range $[0, 1]$ for different \mathcal{C} and \mathcal{R} ; this is done so that α will properly balance the two, and to stabilize training of the GNN policy. The values used are $w_p = (\max_{i,j} T_{ij})^{-1}$ and $w_o = (S \max_{i,j} T_{ij})^{-1}$, where T is an $n \times n$ matrix of shortest-path driving times between every node pair.

4 NEURAL NET HEURISTICS

4.1 Learned Constructor

In order to learn heuristics for transit network design, we first train a neural net policy $\pi_\theta(a|s)$, parameterized by θ , to maximize the cumulative return G_t on the construction MDP described in subsection 3.1. By then following this policy on the MDP for some city \mathcal{C} , randomly sampling a_t at each step with probabilities given by $\pi(\cdot|s_t)$, we can obtain a transit network \mathcal{R} for that city. We refer to this learned policy as the Learned Constructor (LC). The policy can be used for planning in one of two modes: stochastic mode, in which each action a_t is randomly sampled from the distribution $\pi_\theta(\cdot|s_t)$, and greedy mode, in which each action is deterministically (“greedily”) chosen as the highest-scored under the policy, $a_t = \max_{a \in \mathcal{A}} \pi(a|s_t)$.

The central component of the policy net is a graph attention net (GAT) Brody et al. (2021) which treats the city as a fully-connected graph on the nodes \mathcal{N} . Each node has an associated feature vector \mathbf{x}_i , and each edge a feature vector \mathbf{e}_{ij} , that contain information about location, demand, existing transit connections, and the street edge (if one exists) between i and j . We note that a graph attention net operating on a fully-connected graph has close parallels to a Transformer model Vaswani et al. (2017), but unlike Transformers this architecture enables the use of edge features that describe known relationships between elements.

The GAT outputs node embeddings \mathbf{y}_i , which are operated on by one of two policy “heads”, depending on the timestep: NN_{ext} for choosing among extensions when the timestep t is odd, and NN_{halt} for deciding whether to halt when t is even. Figure 2 is a schematic illustration of the function of each of these three components in the route-planning MDP. The full details of the neural architecture are presented in Appendix A. We have released the code for our method and experiments to the public².

4.1.1 Training

Following the work of Kool et al. (2019), we train the policy net using REINFORCE with baseline, a policy gradient method proposed by Williams (1992), and set $\gamma = 1$. Since, by construction, the reward is 0 except at the final planning step, this implies the return G_t is the same for all steps:

$$G_t = \sum_{t'}^{t_{end}} R_{t'} = -C(\mathcal{C}, \mathcal{R}_{final}) \quad (8)$$

² Available at https://www.cim.mcgill.ca/~mrl/hgrepo/transit_learning/

The learning signal for each action a_t is $G_t - b(s_t)$, where the baseline $b(s_t)$ is a learned quantity that estimates the average G_t achieved by π_θ starting in state s_t . Differing from Kool et al. (2019), we compute the baseline at each step using a small Multi-Layer Perceptron (MLP) neural net separate from the policy network π_θ . This baseline net is trained to predict G_t based on cost weight parameter α and statistics of the city \mathcal{C} .

We train the policy on a dataset of synthetic cities. We sample a different $\alpha \sim [0, 1]$ for each city, while holding S, n, MIN, MAX , and the constraint weight β constant across training. The values of these parameters used are presented in Table 7. For each batch, a full MDP episode is run on the cities in the batch, $C(\mathcal{C}, \mathcal{R})$ is computed across the batch, and back-propagation and weight updates are applied to both the policy net and the baseline net.

To construct a synthetic city for the training dataset, we first generate its nodes and street network using one of these processes chosen at random:

- 4-nn: Sample n random 2D points uniformly in a square to give \mathcal{N} . Add street edges to each node i from its four nearest neighbours.
- 4-grid: Place n nodes in a rectangular grid as close to square as possible. Add edges from each node to its horizontal and vertical neighbours.
- 8-grid: The same as the above, but also add edges between diagonal neighbours.
- Voronoi: Sample m random 2D points, and compute their Voronoi diagram Fortune (1995). Take the shared vertices and edges of the resulting Voronoi cells as \mathcal{N} and \mathcal{E}_s . m is chosen so $|\mathcal{N}| = n$.

For each process except Voronoi, each edge in \mathcal{E}_s is then deleted with user-defined probability ρ . If the resulting street graph is not strongly connected, it is discarded and the process is repeated. Nodes are sampled in a $30\text{km} \times 30\text{km}$ square, and a fixed vehicle speed of $v = 15\text{m/s}$ is assumed to compute street edge weights $\tau_{ij} = \|(x_i, y_i) - (x_j, y_j)\|_2 / v$. Finally, we generate the OD matrix D by setting diagonal demands $D_{ii} = 0$ and uniformly sampling off-diagonal elements D_{ij} in the range $[60, 800]$.

To generate training data, we follow the general procedure used to generate the synthetic cities in the Mumford benchmark dataset Mumford (2013b). \mathcal{N} is generated by sampling n 2D points in a 30 km by 30 km square. The relationship between n and $n_e = |\mathcal{E}_s|$ in Mumford’s cities approximately $n_e = 3.6 * n - 34$, so we make this the desired number of edges. To generate \mathcal{E}_s , we start with the minimum spanning tree of the nodes in \mathcal{N} , and then add edges (i, j, t_{ij}) to this graph in ascending order of $t_{ij} = \|(x_i, y_i) - (x_j, y_j)\|_2$ until n_e is

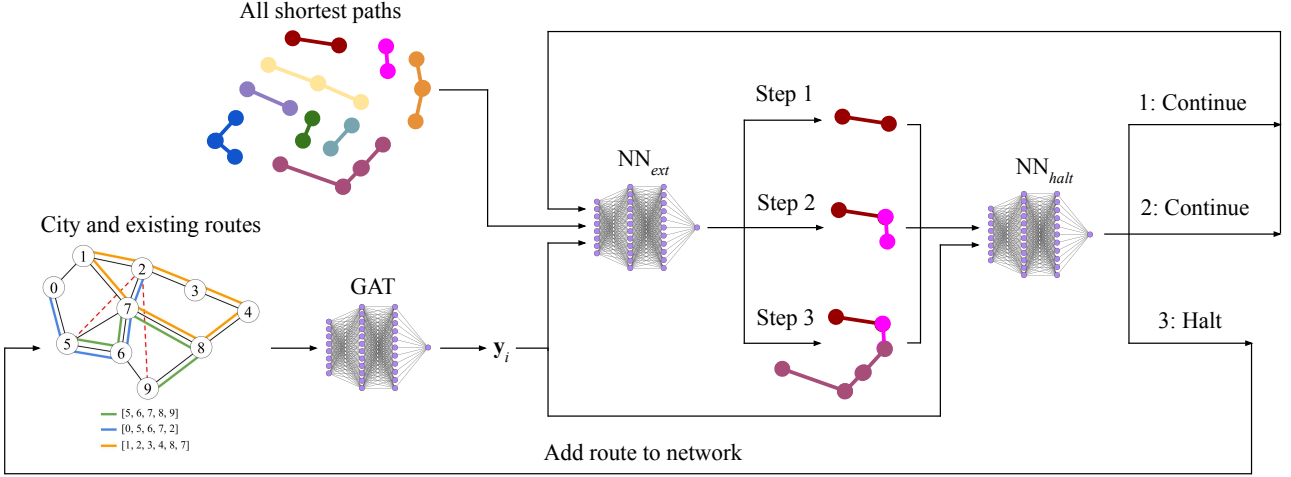


Fig. 2: A schematic of our proposed route-planning method, outlining the route-construction MDP and showing the role of the policy network’s three components: the graph attention net (GAT) backbone, NN_{ext} , and NN_{halt} .

reached. Finally, we generate the OD matrix D by setting diagonal demands $D_{ii} = 0$ and uniformly sampling off-diagonal elements $D_{ij} \sim [60, 800]$.

We train our policies on a dataset of $2^{15} = 32,768$ synthetic cities. We made a 90:10 split of this dataset into training and validation sets. Training progresses in “epochs”, where one epoch corresponds to training the model on one episode over each city in the training set. After each epoch, the policy is run on the validation set, and its average cost is recorded. At the end of training, the parameters θ from the epoch with the lowest average validation cost are returned, giving the final policy π_θ .

All neural net inputs are normalized so as to have unit variance and zero mean across the entire dataset during training. The scaling and shifting normalization parameters are saved as part of the model and applied to new data presented at test time.

4.2 Evolutionary Algorithm

Having trained a learned constructor policy, we may now use it as a low-level heuristic in metaheuristic algorithms. To demonstrate this and see whether it offers any benefit, we here describe an evolutionary algorithm with two mutation operators, and the modified algorithm which replaces one of these mutation operators with one that uses our learned constructor policy.

Our baseline evolutionary algorithm is based on that of Nikolić and Teodorović (2013), with several modifications that we found improved its performance. We chose this algorithm because its ease of implementation and short running times (with appropriate param-

eters) aided prototyping and experimentation, but we note that our learned policies can in principle be used as heuristics in a wide variety of metaheuristic algorithms.

The algorithm operates on a population of B solutions \mathcal{R}_b , and functions by alternating stages of mutation and selection. In the mutation stage, the algorithm applies two mutation operators, “type 1” and “type 2”, each to a subset of the population chosen at random; if the resulting mutation has lower cost, it replaces its “parent”. This proceeds for E steps. In the selection stage, solutions randomly either “die” or “reproduce”, with probabilities inversely related to their cost $C(\mathcal{C}, \mathcal{R}_b)$.

Each mutator begins by selecting, uniformly at random, a route r in the solution and a terminal i on that route. The type-1 mutator then selects a random node $j \neq i$ in \mathcal{N} , and replaces r with the shortest path between i and j . The probability of choosing each node j is proportional to the amount of demand directly satisfied by SP_{ij} . The type-2 mutator chooses with probability p_d to delete i from r ; otherwise, it adds a random node j in i ’s neighbourhood to r (before i if i is the first node in r , and after i if i is the last node in r), making j the new terminal. Following Nikolić and Teodorović (2013), we set the deletion probability $p_d = 0.2$ in our experiments.

The initial population of solutions is constructed by copying a single initial solution, \mathcal{R}_0 , B times. In our prior work (Holliday and Dudek, 2023), we found that using the learned constructor in to plan \mathcal{R}_0 outperformed other methods, so we use this technique here. Specifically, we run the learned constructor in stochastic mode 100 times on a city, generating 100 distinct

transit networks, and then choose the lowest-cost of these as \mathcal{R}_0 . We refer to this procedure as “LC-100”.

The parameters of this algorithm are the population size B , the number of iterations of mutation-selection IT , and the number of mutations per mutation stage E . In addition to these, it takes as input the city \mathcal{C} being planned over, the set of shortest paths through the city’s street graph \mathcal{SP} , and the cost function C . The full procedure is given in 1. We refer to this algorithm as “EA”.

Algorithm 1 Evolutionary Algorithm

```

1: Input:  $\mathcal{C} = (\mathcal{N}, \mathcal{E}_s, D), \mathcal{SP}, C, B, IT, E$ 
2: Construct initial solution  $\mathcal{R}_0$ 
3:  $\mathcal{R}_b \leftarrow \mathcal{R}_0 \forall b \in [1, B]$ 
4:  $\mathcal{R}_{\text{best}} \leftarrow \mathcal{R}_0$ 
5: for  $i = 1$  to  $IT$  do
6:   // Explore around each solution
7:   for  $j = 1$  to  $E$  do
8:     for  $b = 1$  to  $B$  do
9:       if  $b \leq B/2$  then
10:         $\mathcal{R}'_b \leftarrow \text{type\_1\_mod}(\mathcal{R}_b)$ 
11:       else
12:         $\mathcal{R}'_b \leftarrow \text{type\_2\_mod}(\mathcal{R}_b)$ 
13:       if  $C(\mathcal{C}, \mathcal{R}'_b) < C(\mathcal{C}, \mathcal{R}_b)$  then
14:         $\mathcal{R}_b \leftarrow \mathcal{R}'_b$ 
15:   Randomly reorder solutions  $\mathcal{R}_b$  in the population
16:   // Decide which solutions survive and reproduce
17:    $C_{\text{max}} \leftarrow \max_b C(\mathcal{C}, \mathcal{R}_b)$ 
18:    $C_{\text{min}} \leftarrow \min_b C(\mathcal{C}, \mathcal{R}_b)$ 
19:   for  $b = 1$  to  $B$  do
20:     if  $C(\mathcal{C}, \mathcal{R}_b) < C(\mathcal{C}, \mathcal{R}_{\text{best}})$  then
21:       $\mathcal{R}_{\text{best}} \leftarrow \mathcal{R}_b$ 
22:       $O_b \leftarrow \frac{C_{\text{max}} - C_b}{C_{\text{max}} - C_{\text{min}}}$ 
23:       $s_b \sim \text{Bernoulli}(1 - e^{-O_b})$ 
24:       $p_b \leftarrow \frac{O_b s_b}{\sum_{b'} O_{b'} s_{b'}}$ 
25:   if  $\exists b \in [1, B]$  s.t.  $s_b = 1$  then
26:     for  $b = 1$  to  $B$  do
27:       if  $s_b = 0$  then
28:         $k \sim P(K)$ , where  $P(K = b') = p_{b'}$ 
29:         $\mathcal{R}_b \leftarrow \mathcal{R}_k$ 
30: return  $\mathcal{R}_{\text{best}}$ 

```

We note that Nikolić and Teodorović (2013) describe theirs as a “bee colony optimization” algorithm. As noted in Sörensen (2015), “bee colony optimization” is in fact a relabelling of the evolutionary-algorithm metaheuristic: the two are functionally identical. To avoid the profusion of unnecessary terminology, we here describe the algorithm as an evolutionary algorithm.

Our neural evolutionary algorithm NEA differs from EA only in that the type-1 mutator is replaced with a “neural mutator”. This mutator selects a route $r \in \mathcal{R}_b$ at random, deletes it from \mathcal{R}_b , and then rolls out our learned policy π_θ starting from $\mathcal{R}_b \setminus r$, generating one new route r' which is then added to \mathcal{R}_b . The algorithm

is otherwise unchanged. We replace the type-1 mutator because its action space (replacing one route by a shortest path) is a subset of the action space of the neural mutator (replacing one route by a new route composed of shortest paths), while the type-2 mutator’s action space is quite different. In this way, π_θ , which was trained as a construction policy, is applied to aid in an improvement method.

5 MUMFORD EXPERIMENTS

We first evaluated our method on the Mandl (1980) and Mumford (2013b) city datasets, two popular benchmarks for evaluating NDP algorithms (Mumford, 2013a; John et al., 2014; Kılıç and Gök, 2014; Ahmed et al., 2019). The Mandl dataset is one small synthetic city, while the Mumford dataset consists of four synthetic cities, labelled Mumford0 through Mumford3, and it gives values of S , MIN , and MAX to use when benchmarking on each city. The values n , S , MIN , and MAX for Mumford1, Mumford2, and Mumford3 are taken from three different real-world cities and their existing transit networks, giving the dataset a degree of realism. Details of these benchmarks are given in Table 1.

In all of our experiments, we set the transfer penalty p_T used to compute average trip time C_p to $p_T = 300s$ (five minutes). This value is a reasonable estimate of a passenger’s preference for avoiding transfers versus saving time; it is widely used by other methods when evaluating on these benchmarks (Mumford, 2013a), so using this same value of p_T allows us to directly compare our results with other results on these benchmarks.

5.1 Comparison with Baseline Evolutionary Algorithm

We run each algorithm under consideration on all five of these synthetic cities over eleven different values of α , ranging from 0.0 to 1.0 in increments of 0.1. This lets us observe how well the different methods perform under a range of possible preferences, from the extremes of the operator perspective ($\alpha = 0.0$) and passenger perspective ($\alpha = 1.0$) to a range of intermediate perspectives. The constraint weight $\beta = 5.0$ in all experiments, the same value used in training the policies. We found that this β was sufficient: none of the transit networks produced in our experiments violated any of the constraints in section 3.

We perform ten runs of each method with ten different random seeds. For algorithms that make use of a learned constructor policy, ten such policies were trained with the same set of random seeds (but using

Table 1: Statistics of the five benchmark problems used in our experiments.

City	# nodes n	# street edges $ \mathcal{E}_s $	# routes S	MIN	MAX	Area (km ²)
Mandl	15	20	6	2	8	352.7
Mumford0	30	90	12	2	15	354.2
Mumford1	70	210	15	10	30	858.5
Mumford2	110	385	56	10	22	1394.3
Mumford3	127	425	60	12	25	1703.2

the same training dataset), and each was used in the run with the corresponding random seed. We report the mean and standard deviation of total route time C_o and average trip time C_p for each run.

We first compared our neural evolutionary algorithm (NEA) with our baseline evolutionary algorithm (EA). We also compare both with the initial solutions from LC-100, to see how much each of EA and NEA improve the solution. In the EA and NEA runs, the same parameter settings of $B = 10, IT = 400, E = 10$ were used. Table 2 gives statistics of the final cost achieved by each algorithm on Mandl and the four Mumford cities for the operator perspective ($\alpha = 0.0$), the passenger perspective ($\alpha = 1.0$), and a balanced perspective ($\alpha = 0.5$). We see that on Mandl, the smallest of the five cities, EA and NEA perform virtually identically for the operator and passenger perspectives, while NEA offers a slight improvement for the balanced perspective. But for the larger cities of the Mumford dataset, NEA performs considerably better than EA for both the operator and balanced perspectives.

For the passenger perspective NEA’s advantage over EA is smaller, but it still outperforms EA on Mumford1 and Mumford3 and performs comparably on Mumford2. On Mumford3, the largest of the five cities, NEA solutions EA have 14% lower average cost for the passenger perspective and 6% lower for the balanced perspective. For the operator perspective, the difference is much less significant: NEA’s solutions have 1% lower average cost, but the average costs of NEA and EA are within one standard deviation of each other.

Figure 3 displays the values of average trip time C_p and total route time C_o achieved by each algorithm on the three largest Mumford cities, the three which are each based on a real city’s statistics, over the full range of α values. There is a necessary trade-off between these two values, and as we expect, as α increases, we observe that C_o increases while C_p decreases for each method. We also observe that for intermediate values of α , NEA pushes C_o much lower than LC-100, at the cost of increases in C_p . This behaviour is desirable, because as the figure shows, NEA achieves an overall larger range of outcomes than LC-100 - for any solution from LC-100, there is some value of α for which NEA produces a

strictly dominant solution. Figure 3 also shows results for an additional algorithm, LC-40k, which will be discussed in subsection 5.2.

On all three cities, we observe a common pattern: EA and NEA perform very similarly at $\alpha = 1.0$ (the leftmost point on each curve), but a significant performance gap forms as α decreases - consistent with what is shown by Table 2. We also observe that LC-100 performs better in terms of C_p than C_o , with its points clustered higher and more leftwards than most of the points with corresponding α values on the other curves. Both EA and NEA make only very small decreases in C_p on LC-100’s initial solutions at $\alpha = 1.0$, and they do so by increasing C_o considerably.

5.2 Ablation Studies

To better understand the contribution of various components of our method, we performed a set of three ablation studies, described below. These were conducted over the three realistic Mumford cities and over the same range of α values as in subsection 5.1.

5.2.1 Effect of number of samples

We observe that over the course of the evolutionary algorithm, with the parameter settings $B = 10, IT = 400, E = 10$, a total of $B \times IT \times E = 40,000$ different transit networks are considered. By comparison, LC-100 only considers 100 solutions. It could be that NEA’s superiority to LC-100 is only due to its considering more solutions. To test this, we ran LC-40k, in which we sample 40,000 solutions from the learned constructor, and picks the lowest-cost of those. Comparing LC-100 and LC-40k in Figure 3, we see that across all three cities and all values of α , LC-40k performs very similarly to LC-100, improving on it only slightly in comparison with the improvement given by EA or NEA. From this we conclude that the number of solutions considered is not on its own an important factor in EA’s and NEA’s performance: much more important is the evolutionary algorithm that guides the search through solution space.

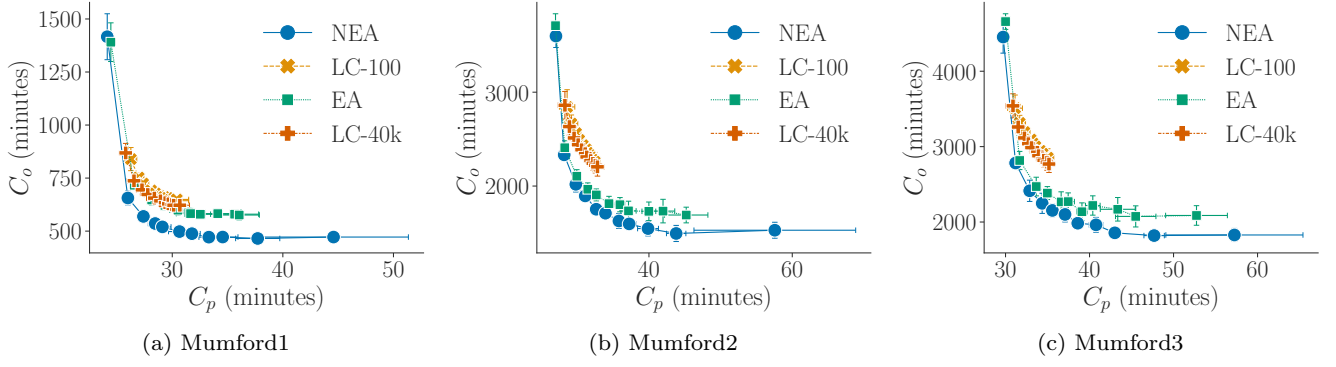


Fig. 3: Trade-offs between average trip time C_p (on the x-axis) and total route time C_o (on the y-axis), across values of α evenly spaced over the range $[0, 1]$, from $\alpha = 0.0$ at right to 1.0 at left, for transit networks from LC-100, LC-40k, EA, and NEA. Points are the average over 10 random seeds, and bars around each point indicate one standard deviation. A line links every two points with consecutive α values. Lower values of C_o and C_p are better, so the lower-left direction in each plot represents improvement.

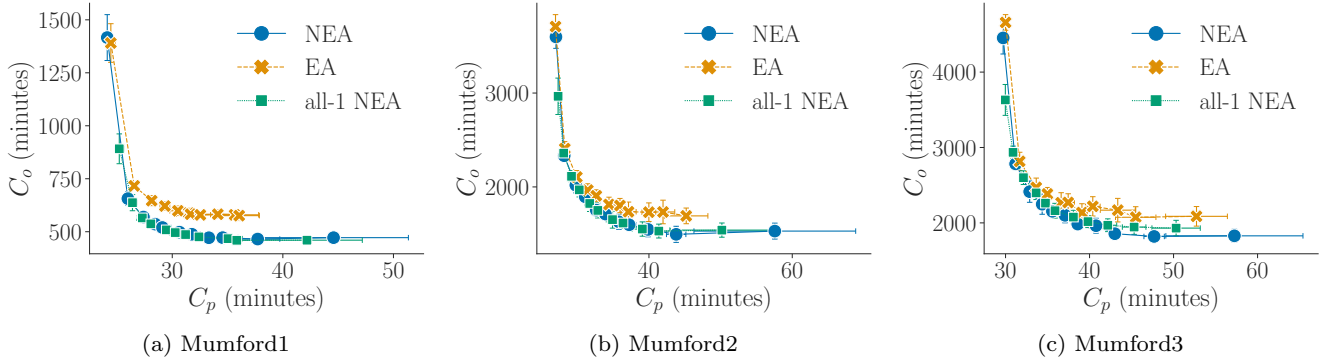


Fig. 4: Trade-offs between average trip time C_p (on the x-axis) and total route time C_o (on the y-axis) achieved by all-1 NEA, plotted along with EA and NEA for comparison.

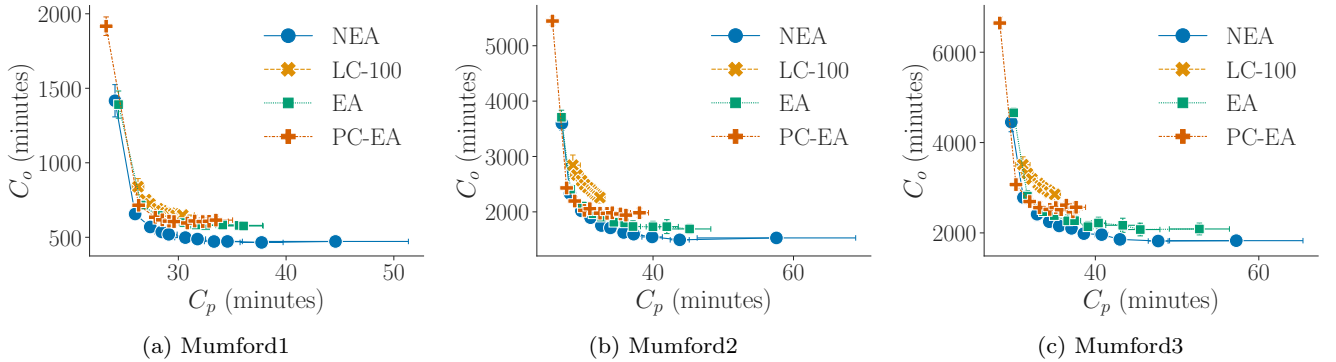


Fig. 5: Trade-offs between average trip time C_p (on the x-axis) and total route time C_o (on the y-axis) achieved by PC-EA, plotted along with LC-100, EA, and NEA for comparison.

Table 2: Final cost $C(\alpha, \mathcal{C}, \mathcal{R})$ achieved baseline experiments for three different α values. Values are averaged over ten random seeds; the \pm value is the standard deviation of $C(\alpha, \mathcal{C}, \mathcal{R})$ over the seeds.

α	Method	Mandl	Mumford0	Mumford1	Mumford2	Mumford3
0.0	LC-100	0.677 ± 0.014	0.801 ± 0.020	1.950 ± 0.028	1.523 ± 0.067	1.560 ± 0.065
	EA	0.675 ± 0.010	0.747 ± 0.012	1.757 ± 0.052	1.140 ± 0.056	1.140 ± 0.071
	NEA	0.675 ± 0.010	0.744 ± 0.019	1.430 ± 0.044	1.030 ± 0.057	0.999 ± 0.047
0.5	LC-100	0.551 ± 0.008	0.895 ± 0.015	1.335 ± 0.012	1.100 ± 0.015	1.095 ± 0.017
	EA	0.545 ± 0.007	0.843 ± 0.015	1.242 ± 0.026	0.936 ± 0.024	0.928 ± 0.031
	NEA	0.541 ± 0.007	0.835 ± 0.009	1.103 ± 0.012	0.896 ± 0.018	0.878 ± 0.025
1.0	LC-100	0.333 ± 0.007	0.725 ± 0.025	0.597 ± 0.012	0.539 ± 0.020	0.511 ± 0.014
	EA	0.317 ± 0.002	0.607 ± 0.008	0.556 ± 0.009	0.509 ± 0.009	0.492 ± 0.008
	NEA	0.318 ± 0.004	0.615 ± 0.008	0.548 ± 0.005	0.510 ± 0.009	0.487 ± 0.007

5.2.2 Contribution of type-2 mutator

We now consider the impact of the type-2 mutator on NEA. This operator is the same between EA and NEA and is not a learned function. To understand how important it is to NEA’s performance, we ran “all-1 NEA”, a variant of NEA in which only the neural mutator is used, and not the type-2 mutator. The results are shown in Figure 4, along with the same curves for LC-100 and NEA as in Figure 3, for comparison. It is clear that NEA and all-1 NEA perform very similarly in most scenarios. The differences are most notable at the extreme values of α (at either end of each curve), where we see that all-1 NEA underperforms NEA, achieving higher values of the relevant cost function component; but at intermediate α values, NEA and all-1 NEA’s trip-time-versus-operating-cost curves overlap. It appears that the minor adjustments to existing routes made by the type-2 mutator are more important at extremes of α , where the neural net policy has been pushed to the extremes of its behaviour.

While the type-2 mutator’s contribution is small, it does help performance at extreme values and does not appear to worsen it at intermediate values, so it is worth retaining as a component of the algorithm.

5.2.3 Importance of learned heuristics

We observe that the type-1 mutator used in EA and the neural mutator used in NEA differ in the space of changes each is capable of making. The type-1 mutator can only add shortest paths as routes, while the neural mutator may compose multiple shortest paths into its new routes. This structural difference, and not the quality of heuristics learned by the policy π_θ , may be what gives NEA its advantage over EA.

To test this conjecture, we ran a variant of NEA in which the learned policy is replaced by a policy that chooses actions uniformly at random: $\pi_{rand}(a|s_t) =$

$\frac{1}{|\mathcal{A}_t|} \forall a \in \mathcal{A}_t$. We call this the Path-combining EA (PC-EA). Since we wanted to gauge the performance of this variant in isolation from the learned policy, we did not use LC-100 with a learned policy to generate the initial solution \mathcal{R}_0 . Instead, we used this random policy in LC-100 to generate \mathcal{R}_0 for PC-EA.

The results are shown in Figure 5, along with the same LC-100, EA, and NEA curves as in Figure 3. We see that for most values of α , PC-EA performs less well than both EA and NEA. On the other hand, at the extreme of $\alpha = 0.1$ it performs better than both NEA and EA, decreasing average trip time C_p to about two minutes less than NEA on average. PC-EA’s poor performance at low α makes sense: its ability to replace routes with composites of shortest paths biases it towards making longer routes, moreso than EA. This is an advantage at $\alpha = 1.0$ but a disadvantage at $\alpha = 0.0$ (and, as we observe here, at intermediate α). It is interesting, though, that PC-EA outperforms NEA at $\alpha = 1.0$, as these two share the same space of possible actions. We would expect that if this action space enables the degree of performance shown by PC-EA, then the neural net policy used in NEA should be able to learn to reach that performance as well. Yet somehow in this scenario it fails to do so. Nonetheless, NEA performs better overall than PC-EA, and so we leave the exploration of this mystery to future work. For now we merely note that composing shortest paths appears to be a very useful heuristic for route construction in its own right, even when done purely randomly.

5.3 Comparisons with prior work

During the experiments of subsection 5.1, we observed that after 400 iterations NEA’s best-solution quality was still improving. In order to make a fairer comparison with other methods from the literature on the Mandl and Mumford benchmarks, we performed

a further set of experiments where we ran NEA with $IT = 4,000$ instead of 400, for $\alpha = 0.0$ and $\alpha = 1.0$. In addition, because we observed better performance from PC-EA for α near 1.0, we also ran PC-EA with $IT = 4,000$ for $\alpha = 1.0$, and we include these results as well.

Table 3 and Table 4 present the results of these experiments on Mandl and the four Mumford cities, alongside results reported on these cities in comparable recent work. All results we report for NEA and PC-EA are averaged over ten runs with different random seeds; the same set of ten trained models used in the experiments of subsection 5.1 and subsection 5.2 are used here in NEA. Results for other methods are as reported by their authors. In addition to average trip time C_p and total route time C_o , the tables present d_0 , d_1 , d_2 , and d_{un} . For $i \in [0, 2]$, d_i is the percentage of all passenger trips that require i transfers between transit routes; while d_{un} is the percentage of trips that require more than 2 transfers ($d_{un} = 100 - (d_0 + d_1 + d_2)$).

In these comparisons, we do not include results from Ahmed et al. (2019). While they report impressive results on these benchmarks, they do not provide the values used for the two parameters to their algorithm. In our earlier work Holliday and Dudek (2023), theirs was one of several methods we implemented in order to test our proposed initialization scheme. We discovered parameter values on our own that gave results comparable to other work up to 2019, but unfortunately after much effort and correspondence with one of the authors of Ahmed et al. (2019), we were unable to replicate their reported results. For this reason, we do not include their reported results here.

On a desktop computer with a 2.4 GHz Intel i9-12900F processor and an NVIDIA RTX 3090 graphics processing unit (used to accelerate our neural net computations), NEA takes about 3 hours for each run on Mumford3, the largest environment, while the PC-EA runs take about 2.5 hours. By comparison, John et al. (2014) and Hüsselmann et al. (2023)’s NSGA-II variant, which each employ a genetic algorithm with a population of 200 solutions, take more than two days to run on Mumford3. Kılıç and Gök (2014) report that their procedure takes eight hours just to construct the initial solution for Mumford3, and don’t report the running time for the subsequent optimization. Hüsselmann et al. (2023)’s DBMOSA variant, meanwhile, takes 7 hours and 52 minutes to run on Mumford3.

These reported running times are not directly comparable as the experiments were not run on identical hardware, but the differences are broadly indicative of the differences in speed of these methods. The running times of these methods is mainly a function of

the metaheuristic algorithm used, rather than the mutation operators that alter solutions at each step. Genetic algorithms like NSGA-II, with large populations as used in some of these methods, are known to be very time-consuming because of the large number of solutions they must modify and evaluate at each step. But their search of solution space is correspondingly more exhaustive than single-solution methods such as simulated annealing, or an evolutionary algorithm with a small population ($B = 10$) as we use in our own experiments. It is therefore to be expected that they would achieve lower final costs in exchange for their greater run-time. We are interested here in the quality of the low-level heuristics we propose, rather than the metaheuristic algorithm, and this must be kept in mind as we discuss the results of this section.

Table 3 shows the passenger perspective results. On each city except Mumford1, the NSGA-II variant of Hüsselmann et al. (2023) has the best final performance; it is also among the most time-consuming of the algorithms reported on here. PC-EA and NEA both perform poorly on the smallest two cities, Mandl and Mumford0, but their relative performance improves as the size of the city increases. On both Mumford2 and Mumford3, PC-EA’s performance is very close to that of Hüsselmann et al. (2023)’s NSGA-II, and better than all other methods listed, despite the relatively under-powered metaheuristic that drives it. In particular, it outperforms Hüsselmann et al. (2023)’s DBMOSA, which uses the same low-level heuristics as the NSGA-II with a faster but less-exhaustive metaheuristic. That PC-EA exceeds its performance on Mumford2 and Mumford3 is evidence that the low-level heuristics used in PC-EA are better for the passenger perspective than those proposed by Hüsselmann et al. (2023). This is especially the case given that DBMOSA is still a more powerful metaheuristic, making use of a hyper-heuristic to adapt the probability that each of its low-level heuristics will be applied over the run. By contrast, PC-EA always applies both of its heuristics equally often.

NEA does not perform as well as PC-EA on (aligning with what we observed in subsection 5.2), but still shows good performance on Mumford2 and 3, here outperforming all of these methods that were published prior to 2022.

Table 4 makes the same comparison for the operator perspective. Kılıç and Gök (2014) does not report results for the operator perspective and as such we do not include it in this table. Similarly to the passenger-perspective results, our methods underperform on the smallest cities (Mandl and Mumford0) but perform well on larger ones. Strikingly, despite NEA’s under-powered metaheuristic, it achieves the lowest value of total route

City	Method	$C_p \downarrow$	$C_o \downarrow$	$d_0 \uparrow$	d_1	d_2	$d_{un} \downarrow$
Mandl	Mumford (2013a)	10.27	221	95.38	4.56	0.06	0
	John et al. (2014)	10.25	212	-	-	-	-
	Kılıç and Gök (2014)	10.29	216	95.5	4.5	0	0
	Hüsselmann et al. (2023) DBMOSA	10.27	179	95.94	3.93	0.13	0
	Hüsselmann et al. (2023) NSGA-II	10.19	197	97.36	2.64	0	0
	NEA	10.42	185	92.49	7.24	0.27	0
	PC-EA	10.32	194	94.15	5.74	0.11	0
Mumford0	Mumford (2013a)	16.05	759	63.2	35.82	0.98	0
	John et al. (2014)	15.4	745	-	-	-	-
	Kılıç and Gök (2014)	14.99	707	69.73	30.03	0.24	0
	Hüsselmann et al. (2023) DBMOSA	15.48	431	65.5	34.5	0	0
	Hüsselmann et al. (2023) NSGA-II	14.34	635	86.94	13.06	0	0
	NEA	15.84	559	52.19	42.41	5.35	0.05
	PC-EA	14.96	722	63.21	36.36	0.43	0
Mumford1	Mumford (2013a)	24.79	2038	36.6	52.42	10.71	0.26
	John et al. (2014)	23.91	1861	-	-	-	-
	Kılıç and Gök (2014)	23.25	1956	45.1	49.08	5.76	0.06
	Hüsselmann et al. (2023) DBMOSA	22.31	1359	57.14	42.63	0.23	0
	Hüsselmann et al. (2023) NSGA-II	21.94	1851	62.11	37.84	0.05	0
	NEA	24.08	1414	33.58	45.44	18.51	2.47
	PC-EA	23.01	1924	39.57	49.66	10.46	0.32
Mumford2	Mumford (2013a)	28.65	5632	30.92	51.29	16.36	1.44
	John et al. (2014)	27.02	5461	-	-	-	-
	Kılıç and Gök (2014)	26.82	5027	33.88	57.18	8.77	0.17
	Hüsselmann et al. (2023) DBMOSA	25.65	3583	48.07	51.29	0.64	0
	Hüsselmann et al. (2023) NSGA-II	25.31	4171	52.56	47.33	0.11	0
	NEA	26.63	3973	32.42	48.89	17.48	1.21
	PC-EA	25.45	5536	41.18	52.96	5.84	0.02
Mumford3	Mumford (2013a)	31.44	6665	27.46	50.97	18.79	2.81
	John et al. (2014)	29.5	6320	-	-	-	-
	Kılıç and Gök (2014)	30.41	5834	27.56	53.25	17.51	1.68
	Hüsselmann et al. (2023) DBMOSA	28.22	4060	45.07	54.37	0.56	0
	Hüsselmann et al. (2023) NSGA-II	28.03	5018	48.71	51.1	0.19	0
	NEA	29.27	5155	30.36	51.01	17.43	1.2
	PC-EA	28.09	6830	38.6	57.02	4.35	0.03

Table 3: Passenger-perspective results. C_p is the average passenger trip time. C_o is the total route time. d_i is the number of trips satisfied with number of transfers i , while d_{un} is the number of trips satisfied with 3 or more transfers. Arrows next to each quantity indicate which of increase or decrease is desirable. Bolded values in C_p , d_0 , and d_{un} columns are the best on that environment.

time C_o out of all methods on Mumford1, 2, and 3, improving even on Hüsselmann et al. (2023)’s NSGA-II with its much higher computational cost. Evidently, the learned policy functions very well as a low-level heuristic at low values of α , where the premium is on keeping routes short, though less well when the premium is on shortening passenger trips.

The percentage-per-transfers metrics d_0 to d_{un} reveal that both PC-EA and NEA favour higher numbers of transfers relative to most of the other methods, particularly Hüsselmann et al. (2023). This is true for both the passenger and operator perspectives. For the operator perspective, this matches our intuitions: shorter routes necessitate more transfers to achieve full coverage. But we were surprised to observe this in the passen-

ger perspective case as well. Compared to Hüsselmann et al. (2023)’s DBMOSA, PC-EA achieves lower mean passenger travel time on Mumford2 and Mumford3 for the passenger perspective, despite the fact that it requires more passenger trips to make 1 and 2 transfers. Still, PC-EA does give fewer transfers overall than NEA, which matches our intuition that fewer transfers should result in lower average trip time C_p .

It seems that the process of compositing shortest paths to form routes biases those routes towards directness and efficiency, to a degree that outweighs the cost imposed by having more transfers. Each transfer is less impactful on riders if the routes they’re transferring between are each more direct. Meanwhile, since both the learned heuristic of NEA and the unlearned

City	Method	$C_o \downarrow$	C_p	$d_0 \uparrow$	d_1	d_2	$d_{un} \downarrow$
Mandl	Mumford (2013a)	63	15.13	70.91	25.5	2.95	0.64
	John et al. (2014)	63	13.48	-	-	-	-
	Hüsselmann et al. (2023) DBMOSA	63	13.55	70.99	24.44	4.00	0.58
	Hüsselmann et al. (2023) NSGA-II	63	13.49	71.18	25.21	2.97	0.64
	NEA	67	14.19	56.80	32.02	10.66	0.53
Mumford0	Mumford (2013a)	111	32.4	18.42	23.4	20.78	37.40
	John et al. (2014)	95	32.78	-	-	-	-
	Hüsselmann et al. (2023) DBMOSA	98	27.61	22.39	31.27	18.82	27.51
	Hüsselmann et al. (2023) NSGA-II	94	27.17	24.71	38.31	26.77	10.22
	NEA	116	29.47	14.83	31.74	29.12	24.31
Mumford1	Mumford (2013a)	568	34.69	16.53	29.06	29.93	24.66
	John et al. (2014)	462	39.98	-	-	-	-
	Hüsselmann et al. (2023) DBMOSA	511	26.48	25.17	59.33	14.54	0.96
	Hüsselmann et al. (2023) NSGA-II	465	31.26	19.70	42.09	33.87	4.33
	NEA	448	43.22	14.15	22.44	23.53	39.87
Mumford2	Mumford (2013a)	2244	36.54	13.76	27.69	29.53	29.02
	John et al. (2014)	1875	32.33	-	-	-	-
	Hüsselmann et al. (2023) DBMOSA	1979	29.91	22.77	58.65	18.01	0.57
	Hüsselmann et al. (2023) NSGA-II	1545	37.52	13.48	36.79	34.33	15.39
	NEA	1446	62.27	8.14	14.60	16.65	60.60
Mumford3	Mumford (2013a)	2830	36.92	16.71	33.69	33.69	20.42
	John et al. (2014)	2301	36.12	-	-	-	-
	Hüsselmann et al. (2023) DBMOSA	2682	32.33	23.55	58.05	17.18	1.23
	Hüsselmann et al. (2023) NSGA-II	2043	35.97	15.02	48.66	31.83	4.49
	NEA	1788	56.04	8.74	15.81	19.86	55.58

Table 4: Operator perspective results. C_p is the average passenger trip time. C_o is the total route time. d_i is the number of trips satisfied with number of transfers i , while d_{un} is the number of trips satisfied with 3 or more transfers. Arrows next to each quantity indicate which of increase or decrease is desirable. Bolded values in C_o , d_0 and d_{un} columns are the best on that environment.

heuristic of PC-EA suffer from high transfer counts, it seems the difference between these and the other results from the literature may be a result of the evolutionary algorithm itself. At any rate, these results are not out of line with those of Mumford (2013a) and Kılıç and Gök (2014) on the largest cities, so we do not consider this a major strike against our heuristics. Indeed, we expect that these results could be improved by explicitly including d_0 in the cost function used to train the neural net policy, and this would reduce the number of transfers achieved by NEA.

6 REAL-WORLD EVALUATION

6.1 Laval Scenario

To assess our method in a realistic problem instance, we applied it to a dataset representing the city of Laval in Quebec, Canada. Laval is a suburb of the major Canadian city of Montreal. As of the 2021 census, it had a total population of 429,555 (Statistics Canada, 2023). Our model of the city of Laval is based on several sources: geographic data on census dissemination ar-

eas for 2021 from Statistics Canada (Statistics Canada, 2021), a map of the street network of the city, an OD dataset (Agence métropolitaine de transport, 2013), and publicly-available GTFS data from 2013 (STL) that describes the existing transit system in the city.

6.1.1 Street graph

The street graph $\mathcal{N}, \mathcal{E}_s$ was derived from the 2021 census dissemination data by taking the centroid of each dissemination area within Laval to be a node in \mathcal{N} , and adding a street edge between any two nodes whose dissemination areas shared a border. To assign drive times t_{ij} , we find all points in the road network within the dissemination areas of i and j , compute the shortest-path driving distance over the road network between each pair of points in i and j , and set t'_{ij} as the median of these driving distances. We do this so that its value will better reflect the real drive times given the existing road network. As our method treats cities as undirected graphs, it expects that $t_{ij} = t_{ji} \forall i, j \in \mathcal{N}$. To enforce this, as a final step we set:

$$t_{ij} = t_{ji} = \max(t'_{ij}, t'_{ji}) \forall i, j \in \mathcal{N} \quad (9)$$

6.1.2 Existing transit

The existing transit system in Laval has 43 bus routes that operate during morning rush hour from 7 to 9 AM. We map each stop on an existing bus route to a node in \mathcal{N} based on which census dissemination area contains the stop. Doing this for all routes gives us a version of the existing transit system that runs over our street graph $\mathcal{N}, \mathcal{E}_s$, allowing us to compare it directly with solutions output by our algorithm. We will refer to this mapped transit system as the STL network, after the city’s transit agency “Société de transport de Laval”.

The numbers of stops on the routes in the STL network range from 2 to 52. To ensure a fair comparison, we set $MIN = 2$ and $MAX = 52$ in the same way when running our algorithm. Unlike the routes in our algorithm’s solutions, many of STL’s routes are not symmetrical (that is, they follow a different path in each direction between terminals), and several are unidirectional (they go only one way between terminals). We maintain the constraints of symmetry and bidirectionality on our own algorithm, but do not enforce them upon the STL network. The only modification we make is that when reporting total route time C_o in this section, we calculate it by summing the travel times of both directions of each route, instead of just one direction as in the preceding sections.

In addition, there is an underground metro line, the Montreal Orange Line, which has three stops in Laval. As with the existing bus lines, we map these three stops to their containing DAs and treat them as an additional bus route. We consider it to be fixed, and we include it in our evaluation both of the STL network and the solutions produced by our algorithm.

6.1.3 Demand matrix

Each entry in the OD dataset corresponds to a trip, and has (lat,lon) coordinates l_o and l_d for the trip’s origin and destination, as well as an “expansion factor” e giving the estimated number of actual trips corresponding to that surveyed trip. It also indicates the mode of travel, such as car, bicycle, or public transit, that was used to make the trip.

To assemble D for Laval, we initialize its entries to 0. Then for each entry in the OD dataset, we find which dissemination area contains each of l_o and l_d , and associate them with the matching nodes i and j in \mathcal{N} . We then update $D_{ij} \leftarrow D_{ij} + e$, so that D has the estimated demand between every pair of census dissemination areas. To enforce symmetric demand, we then assign $D_{ij} \leftarrow \max(D_{ij}, D_{ji}) \forall i, j \in \mathcal{N}$.

Many entries in the OD dataset refer to trips that begin or end in Montreal. For our purposes, we “redirect” all trips that enter or leave Laval and are made by public transit to one of several “crossover points” that we define. These crossover points are the locations of the three Orange Line metro stations in Laval, and the locations of the last or first stop in Laval of each existing bus line that goes between Laval and Montreal. For each trip between Laval and Montreal, we identify the crossover point that has the shortest distance to either of the trip’s endpoints, and replace the Montreal endpoint of the trip by this crossover point. This process was automated with a simple computer script. Our intuition here is that if the Laval end of the trip is close to a transit stop that provides access to Montreal, the rider will choose to cross over to the Montreal transit system as soon as possible, as most locations in Montreal will be easier to access once in the Montreal transit system. Trips that go between Laval and Montreal by means other than public transit are not included in D . The resulting demand matrix D contains 548,159 trips, of which 63,104 are trips between Laval and Montreal that we redirected.

Having done the above, we apply one last filtering step. The STL network does not provide a path between all node-pairs with non-zero demand in the demand matrix D , and so violates constraint 1 of section 3. This is because D at this point includes all trips that were made by any means, including to and from areas that are not served by the STL network, possibly because they are populated by car owners unlikely to use transit if it were available. To ensure a fair comparison between the STL network and our algorithm’s solutions, we set to 0 all entries of D for which the STL network does not provide a path. By doing this, we also cause our system to output transit networks that are “closer” to the existing transit network, in that they satisfy the same travel demand as before. This should reduce the scope of the changes required to go from the existing network to a new one proposed by our system.

This way, we consider only demand that is likely to use transit when it is available, because it corresponds to residents already living close to transit. Table 5 contains the statistics of, and parameters used for, the Laval scenario.

6.2 Enforcing constraint satisfaction

In the experiments on the Mandl and Mumford cities described in section 5, the NEA algorithm consistently produced solutions that did not violate any of the constraints in section 3. However, the Laval scenario is considerably larger than even the largest Mumford scenario

Table 5: Statistics and parameters of the Laval scenario

# nodes n	# street edges $ \mathcal{E}_s $	# demand trips	# routes S	MIN	MAX	Area (km ²)
632	4,544	548,159	43	2	52	520.1

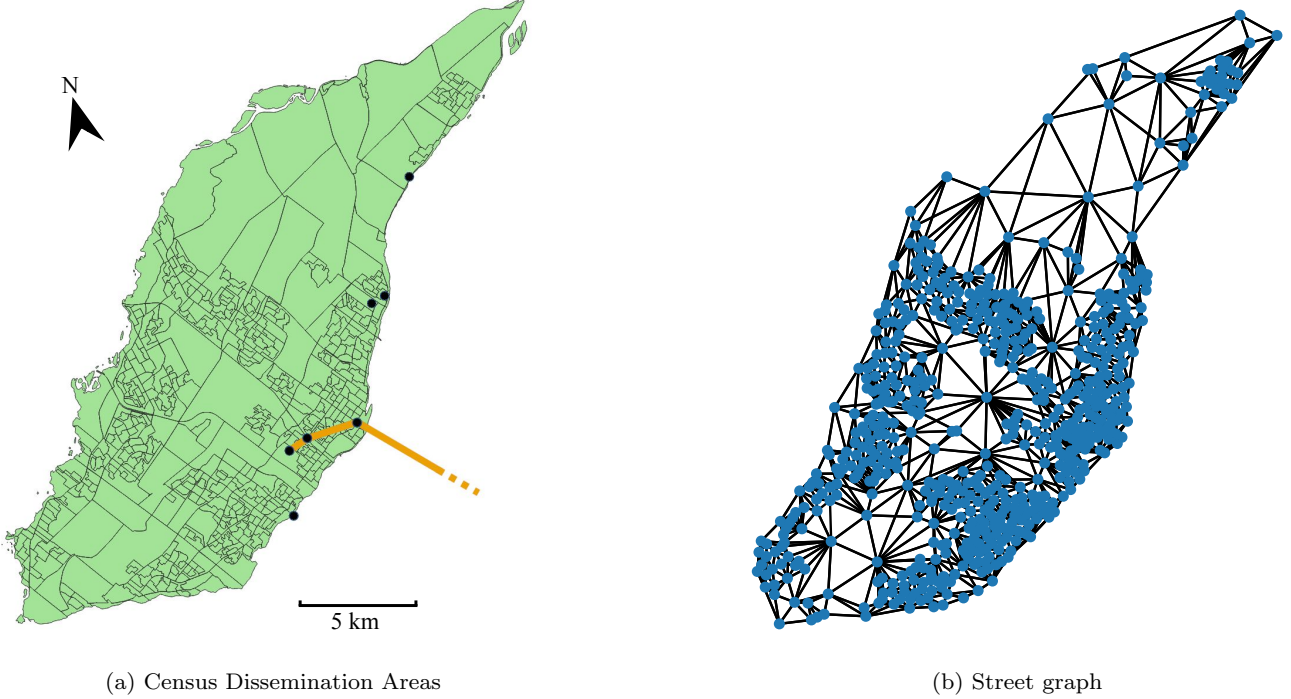


Fig. 6: At left, a map of the census dissemination areas of the city of Laval, with “crossover points” used to remap external demands shown as black circles, as well as the portion of the Orange Line metro that we include. At right, the street graph constructed from these dissemination areas.

(632 nodes versus 127), and in our initial experiments we found that both EA and NEA gave solutions that violated constraint 1, providing no transit path for some node pairs (i, j) for which $D_{ij} > 0$. That is, constraint 1 requires that $c_1(\mathcal{R}) = 0$, where $c_1(\mathcal{R})$ is the number of unconnected node-pairs with non-zero demand over transit network \mathcal{R} .

To remedy this, we modified the MDP described in subsection 3.1 to only allow actions that reduce c_1 , if any such action is available. Specifically, the following changes are applied to the action space \mathcal{A}_t whenever $c_1(\mathcal{R}_t) > 0$:

- When the timestep t is even and \mathcal{A}_t would otherwise be $\{\text{continue}, \text{halt}\}$, the halt action is removed from \mathcal{A}_t . This means that while $c_1(\mathcal{R}_t) > 0$, routes cannot be halted if it is possible to continue.
- When t is odd, if \mathcal{A}_t contains any paths that would reduce $c_1(\mathcal{R}_t)$ if added to r_t , paths that would *not* reduce $c_1(\mathcal{R}_t)$ are excluded from \mathcal{A}_t . This means that if it is *possible* to connect some unconnected

demand by extending a route, then *not* doing so is disallowed.

We apply the same changes when the neural mutator in NEA and its variants plans an individual route. We find that by using these changes both when generating the initial solution via LC-100 and during the subsequent NEA run, the resulting solutions have no constraint violations, even when using policy weights θ that were trained without these changes to the MDP. The results reported in this section are obtained using this variant of the MDP.

6.3 Results

Some trial runs with $IT = 4,000$ showed that the solution quality stopped improving after 2,700 iterations, so to save time we ran our final NEA and PC-EA experiments on Laval with $IT = 3,000$. Other parameters are the same as in the Mumford experiments: $B = 10$, $E = 10$, and transfer penalty $p_T = 300s$. We perform

α	Method	C_p	C_o	d_0	d_1	d_2	d_{un}
	STL	124.61	23954	14.48	22.8	20.88	41.83
0.0	LC-100	88.83	21893	14.19	23.45	23.58	38.78
	NEA	96.65	19624	14.22	23.57	23.63	38.57
	PC-EA	67.67	31907	16.56	32.94	29.06	21.44
0.5	LC-100	79.32	24124	14.88	24.87	24.53	35.72
	NEA	82.55	20978	14.40	24.44	24.76	36.41
	PC-EA	67.40	31784	16.33	33.35	28.99	21.33
1.0	LC-100	66.49	32270	16.35	29.77	26.04	27.85
	NEA	59.23	45382	20.99	34.48	26.71	17.82
	PC-EA	57.42	49016	22.89	39.39	26.33	11.38

Table 6: Performance of STL network, and our system’s networks at three α values. Bolded values are best for a given α . C_p is the average passenger trip time. C_o is the total route time. d_i is the number of trips satisfied with number of transfers i , while d_{un} is the number of trips satisfied with 3 or more transfers. All values are averaged over ten random seeds, excluding STL which is a fixed network.

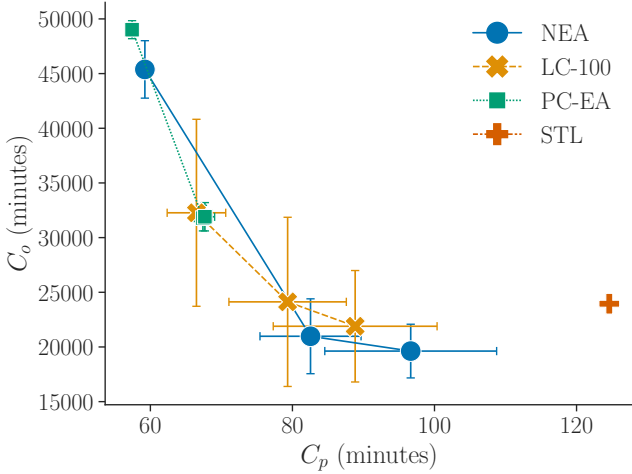


Fig. 7: Trade-offs between average trip time C_p and total route time C_o achieved by LC-100, NEA, PC-EA, for $\alpha = 0.0, 0.5$, and 1.0 , as well as the trade-off for the STL network itself. Each point is a mean value over 10 random seeds, and error bars show one standard deviation. Note that PC-EA’s $\alpha = 0.0$ and 0.5 have nearly identical values (as shown in Table 6), so the corresponding points are stacked in this figure and appear as one point.

three sets of experiments from three perspectives: operator ($\alpha = 0.0$), passenger ($\alpha = 1.0$), and balanced ($\alpha = 0.5$). As above, we perform ten runs of each experiment with ten different random seeds and ten different sets of trained policy weights; the same per-seed weights are used as in the previous experiments.

The results of all experiments are shown in Table 6. As the STL’s network is fixed, its metrics are independent of α , so we show it only once. The results for the LC-100 solution that are used to initialize NEA are

presented as well, to show how much improvement the NEA makes over its initial solution. Figure 7 highlights the trade-offs each method achieves between average trip time C_p and total route time C_o , and how they compare to the STL network.

We see that for each value of α , NEA’s network outperforms the STL network: it achieves 54% lower C_p at $\alpha = 1.0$, 18% lower C_o at $\alpha = 0.0$, and at $\alpha = 0.5$, 34% lower C_p and 12% lower C_o . At both $\alpha = 0.0$ and $\alpha = 0.5$, NEA strictly dominates both lower C_p and lower C_o than the existing transit system.

Comparing NEA’s results to LC-100, we see that at $\alpha = 0.0$, NEA decreases C_o and increases C_p relative to LC-100; and for $\alpha = 1.0$, the reverse is true. In both cases, NEA improves over the initial solution on the sole objective being optimized, at the cost of the other, as we would expect. In the balanced case ($\alpha = 0.5$), we see that NEA decreases C_o by 13% while increasing C_p by 4%. This matches what we observed in Figure 3, as discussed in subsection 5.1.

Looking at the transfer percentages d_0, d_1, d_2 , and d_{un} , we see that the overall number of transfers shrinks, with d_1 growing and d_{un} shrinking, as α increases. This is as expected, since fewer transfers usually means shorter passenger travel times. By the same token, PC-EA performs best on these metrics, as it does on average trip time C_p , since the two are causally linked. Notably though, at $\alpha = 0.0$ NEA’s d_0, d_1 , and d_2 are only slightly higher than the STL network’s - the largest increase is in d_2 , by 13% of STL’s value - while d_{un} is less than the STL network’s, meaning that NEA’s output networks let more passengers reach their destination in 2 or fewer transfers than the STL network. In fact, given the very small decrease in d_0 , the increase in d_1 and d_2 mostly comes from passengers who contributed to d_{un} in the STL network; NEA has thus decreased

the average number of transfers. This is a significant improvement, given that at $\alpha = 0.0$ the algorithm is unconcerned with minimizing passenger travel time.

At $\alpha = 0.5$, NEA's d_{un} decreases further and d_0 , d_1 , and d_2 correspondingly increase, though the change in these values from $\alpha = 0.0$ is very small relative to the decrease in C_p . Then from $\alpha = 0.5$ to 1.0, NEA's d_{un} drops by more than half, and its d_0 , d_1 , and d_2 are all markedly increased, especially in d_0 which is 31% greater than STL's d_0 .

The likely aim of Laval's transit agency is to reduce costs while improving service quality, or at least minimizing its decline. The "balanced" case, where $\alpha = 0.5$, is most relevant to that aim. In this balanced case, we find that NEA proposes solutions that reduce total route time by 13% versus the existing STL transit network.

Some simple calculations can help understand the savings this could represent. The approximate cost of operating one of Laval's buses is 200 Canadian dollars (CAD) per hour. Suppose that each route has the same headway (time between bus arrivals) H . Then, the number of buses N_r required by route r is the route's driving time τ_r divided by the headway, $\frac{\tau_r}{H}$. The total number of buses $N_{\mathcal{R}}$ required for a transit network \mathcal{R} is then:

$$N_{\mathcal{R}} = \sum_{r \in \mathcal{R}} N_r = \frac{1}{H} \sum_{r \in \mathcal{R}} \tau_r = \frac{C_o}{H}$$

So the total cost of the system is $200 \text{ CAD} \times N_{\mathcal{R}}$. Assuming a headway of 15 minutes on all routes, that gives a per-hour operating cost of 319,387 CAD for the STL network, while the average operating cost of networks from NEA with $\alpha = 0.5$ is 279,707 CAD. So under these simplifying assumptions, NEA could save the Laval transit agency on the order of 40,000 CAD per hour - savings of more than 12% of costs. This is only a rough estimate: in practice, headways differ between routes, and there may be additional costs involved in altering the routes from the current system, such as from moving or building bus stops. But it shows that NEA, and neural heuristics more broadly, may offer practical savings to transit agencies.

In addition, NEA's balanced-case networks reduce the average passenger trip time by 34% versus the STL network at the same time as reducing costs. They also reduce the number of transfers that passengers have to make, especially reducing the percentage of trips that require three or more transfers from 41.83% to 36.41%. Trips requiring three or more transfers are widely regarded as being so unattractive that riders will not make them (but note that these trips are still included in the calculation of C_p). So NEA's networks may increase overall transit ridership. This not only makes the

system more useful to the city, but also increases the agency's revenue from fares.

These results demonstrate that learned heuristics may be useful in complex real-world transit planning scenarios. They can improve on an existing transit system in multiple dimensions, in a way sensitive to the planner's preference over these dimensions. Transit agencies may be able to use it to "do more with less", offering better service at reduced cost.

We also note that PC-EA achieves lower average trip time C_p than both STL and NEA for all three α values, but at the cost of worsening total route time C_o versus STL in each case. Furthermore, at $\alpha = 1.0$ where we disregard C_o , it achieves only 3% lower C_p than NEA. This suggests that while the path-combining heuristic for assembling routes is indeed helpful on its own, the learned heuristics of the neural net policy contribute significantly to its performance, reinforcing our observations in subsubsection 5.2.3 and subsection 5.3.

In these experiments, the nodes of the graph represent census dissemination areas instead of existing bus stops. So in order to be used in reality, the proposed routes would need to be fitted to the existing locations of bus stops in the dissemination areas, likely making multiple stops within each area. To minimize the costs of the network redesign, it would be necessary to keep stops at most or all stop locations that have shelters, as constructing or moving these may cost tens of thousands of dollars, while stops with only a signpost at their locations can be moved at the cost of only a few thousand dollars. An algorithm for translating our census-level routes to real-stop-level routes, in a way that minimizes cost, is an important next step for making this work applicable. We leave this for future work.

7 CONCLUSIONS

The choice of low-level heuristics has a major impact on the effectiveness of a metaheuristic algorithm, and our results demonstrate that using deep reinforcement learning to learn heuristics can offer substantial improvements over, or alongside with, engineering them directly. They also demonstrate that learned heuristics may be better-suited to optimizing the transit networks of real-world cities than are human-engineered heuristics, potentially allowing transit agencies to reduce costs while improving quality of service. The method we propose here is a simple one, and presents several obvious directions for improvement.

One is that the construction process on which our neural net policy is trained differs from the metaheuristic algorithm (an improvement process) in which it is

deployed. Another is that we learn just one type of heuristic, that for constructing a route from shortest-path segments, though we note that the neural net may be learning multiple distinct heuristics for how to do this under different circumstances. A natural next step would be to train a more diverse set of neural heuristics, perhaps including route-lengthening and -shortening operators, and to do so directly in the context of an improvement process, which may make the learned heuristics more appropriate to that process.

A remaining question is why the random path-combining heuristic used in the PC-EA experiments outperforms the learned heuristic in the extreme of the passenger perspective. As noted in subsection 5.2.3, in principle the neural net should be able to learn whatever policy the random path-combiner is enacting: in the limit, it could learn to give the same probability to all actions when $\alpha = 1.0$. We wish to explore in more depth why this does not occur, and whether changes to the policy architecture or learning algorithm might improve the learned heuristic's performance to match or exceed the random policy's.

The evolutionary algorithm in which we use our learned heuristic was chosen for its speed and simplicity, which aided in implementation and rapid experimentation. But as noted in subsection 4.2, other more costly but state-of-the-art algorithms, like NSGA-II, may allow still better performance to be gained from learned heuristics. Future work should attempt to use learned heuristics like ours in more varied metaheuristic algorithms.

Another promising place where machine learning can be applied is to learn hyper-heuristics for a metaheuristic algorithm. A typical hyper-heuristic, as used by Ahmed et al. (2019) and Hüßelmann et al. (2023), adapts the probability of using each low-level heuristic based on its performance, while the algorithm is running. Instead of the simple methods used in existing work, we would like to train a neural net policy to act as a hyper-heuristic to select among low-level heuristics, given details about the scenario and previous steps taken during the algorithm.

Our aim in this paper was to show whether learned heuristics can be used in a lightweight metaheuristic algorithm to improve its performance. Our results show that they can, and in fact that they give performance competitive with, and in some cases better than, state-of-the-art algorithms using human-engineered heuristics. Our results provide compelling evidence that they may help transit agencies substantially reduce operating costs while delivering better service to riders in real-world scenarios.

References

- Agence métropolitaine de transport, “Enquête origine-destination 2013,” 2013, montreal, QC.
- L. Ahmed, C. Mumford, and A. Kheiri, “Solving urban transit route design problem using selection hyper-heuristics,” *European Journal of Operational Research*, vol. 274, no. 2, pp. 545–559, 2019.
- G. Ai, X. Zuo, G. Chen, and B. Wu, “Deep reinforcement learning based dynamic optimization of bus timetable,” *Applied Soft Computing*, vol. 131, p. 109752, 2022.
- D. Applegate, R. E. Bixby, V. Chvátal, and W. J. Cook, “Concorde tsp solver,” 2001. [Online]. Available: <https://www.math.uwaterloo.ca/tsp/concorde/index.html>
- P. W. Battaglia, J. B. Hamrick, V. Bapst, A. Sanchez-Gonzalez, V. Zambaldi, M. Malinowski, A. Tacchetti, D. Raposo, A. Santoro, R. Faulkner *et al.*, “Relational inductive biases, deep learning, and graph networks,” *arXiv preprint arXiv:1806.01261*, 2018.
- Y. Bengio, A. Lodi, and A. Prouvost, “Machine learning for combinatorial optimization: a methodological tour d’horizon,” *European Journal of Operational Research*, vol. 290, no. 2, pp. 405–421, 2021.
- S. Brody, U. Alon, and E. Yahav, “How attentive are graph attention networks?” 2021. [Online]. Available: <https://arxiv.org/abs/2105.14491>
- J. Bruna, W. Zaremba, A. Szlam, and Y. LeCun, “Spectral networks and locally connected networks on graphs,” *arXiv preprint arXiv:1312.6203*, 2013.
- X. Chen and Y. Tian, “Learning to perform local rewriting for combinatorial optimization,” *Advances in Neural Information Processing Systems*, vol. 32, 2019.
- S. I.-J. Chien, Y. Ding, and C. Wei, “Dynamic bus arrival time prediction with artificial neural networks,” *Journal of transportation engineering*, vol. 128, no. 5, pp. 429–438, 2002.
- J. Choo, Y.-D. Kwon, J. Kim, J. Jae, A. Hottung, K. Tierney, and Y. Gwon, “Simulation-guided beam search for neural combinatorial optimization,” *Advances in Neural Information Processing Systems*, vol. 35, pp. 8760–8772, 2022.
- P. R. d O Costa, J. Rhuggenaath, Y. Zhang, and A. Akcay, “Learning 2-opt heuristics for the traveling salesman problem via deep reinforcement learning,” in *Asian conference on machine learning*. PMLR, 2020, pp. 465–480.
- H. Dai, E. B. Khalil, Y. Zhang, B. Dilikina, and L. Song, “Learning combinatorial optimization algorithms over graphs,” *arXiv preprint arXiv:1704.01665*, 2017.

- A. Darwish, M. Khalil, and K. Badawi, "Optimising public bus transit networks using deep reinforcement learning," in *2020 IEEE 23rd International Conference on Intelligent Transportation Systems (ITSC)*. IEEE, 2020, pp. 1–7.
- M. Defferrard, X. Bresson, and P. Vandergheynst, "Convolutional neural networks on graphs with fast localized spectral filtering," *CoRR*, vol. abs/1606.09375, 2016. [Online]. Available: <http://arxiv.org/abs/1606.09375>
- J. Durán-Micco and P. Vansteenwegen, "A survey on the transit network design and frequency setting problem," *Public Transport*, vol. 14, no. 1, pp. 155–190, 2022.
- D. K. Duvenaud, D. Maclaurin, J. Iparraguirre, R. Bombarell, T. Hirzel, A. Aspuru-Guzik, and R. P. Adams, "Convolutional networks on graphs for learning molecular fingerprints," *Advances in neural information processing systems*, vol. 28, 2015.
- S. Fortune, "Voronoi diagrams and delaunay triangulations," *Computing in Euclidean geometry*, pp. 225–265, 1995.
- Z.-H. Fu, K.-B. Qiu, and H. Zha, "Generalize a small pre-trained model to arbitrarily large tsp instances," in *Proceedings of the AAAI conference on artificial intelligence*, vol. 35, no. 8, 2021, pp. 7474–7482.
- J. Gilmer, S. S. Schoenholz, P. F. Riley, O. Vinyals, and G. E. Dahl, "Neural message passing for quantum chemistry," in *Proceedings of the 34th International Conference on Machine Learning*, ser. Proceedings of Machine Learning Research, D. Precup and Y. W. Teh, Eds., vol. 70. PMLR, 06–11 Aug 2017, pp. 1263–1272. [Online]. Available: <https://proceedings.mlr.press/v70/gilmer17a.html>
- J. Guan, H. Yang, and S. Wirasinghe, "Simultaneous optimization of transit line configuration and passenger line assignment," *Transportation Research Part B: Methodological*, vol. 40, pp. 885–902, 12 2006.
- V. Guihaire and J.-K. Hao, "Transit network design and scheduling: A global review," *Transportation Research Part A: Policy and Practice*, vol. 42, no. 10, pp. 1251–1273, 2008.
- A. Holliday and G. Dudek, "Augmenting transit network design algorithms with deep learning," in *2023 26th IEEE International Conference on Intelligent Transportation Systems (ITSC)*. IEEE, 2023.
- , "A neural-evolutionary algorithm for autonomous transit network design," in *presented at 2024 IEEE International Conference on Robotics and Automation (ICRA)*. IEEE, 2024.
- A. Hottung and K. Tierney, "Neural large neighborhood search for the capacitated vehicle routing problem," *arXiv preprint arXiv:1911.09539*, 2019.
- G. Hüselmann, J. H. van Vuuren, and S. J. Andersen, "An improved solution methodology for the urban transit routing problem," *Computers & Operations Research*, p. 106481, 2023.
- K. A. Islam, I. M. Moosa, J. Mobin, M. A. Nayeem, and M. S. Rahman, "A heuristic aided stochastic beam search algorithm for solving the transit network design problem," *Swarm and Evolutionary Computation*, vol. 46, pp. 154–170, 2019.
- R. Jeong and R. Rilett, "Bus arrival time prediction using artificial neural network model," in *Proceedings. The 7th international IEEE conference on intelligent transportation systems (IEEE Cat. No. 04TH8749)*. IEEE, 2004, pp. 988–993.
- Z. Jiang, W. Fan, W. Liu, B. Zhu, and J. Gu, "Reinforcement learning approach for coordinated passenger inflow control of urban rail transit in peak hours," *Transportation Research Part C: Emerging Technologies*, vol. 88, pp. 1–16, 2018. [Online]. Available: <https://www.sciencedirect.com/science/article/pii/S0968090X18300111>
- M. P. John, C. L. Mumford, and R. Lewis, "An improved multi-objective algorithm for the urban transit routing problem," in *Evolutionary Computation in Combinatorial Optimisation*, C. Blum and G. Ochoa, Eds. Berlin, Heidelberg: Springer Berlin Heidelberg, 2014, pp. 49–60.
- A. Kar, A. L. Carrel, H. J. Miller, and H. T. Le, "Public transit cuts during covid-19 compound social vulnerability in 22 us cities," *Transportation Research Part D: Transport and Environment*, vol. 110, p. 103435, 2022.
- K. Kepaptsoglou and M. Karlaftis, "Transit route network design problem: Review," *Journal of Transportation Engineering*, vol. 135, no. 8, pp. 491–505, 2009.
- M. Kim, J. Park *et al.*, "Learning collaborative policies to solve np-hard routing problems," *Advances in Neural Information Processing Systems*, vol. 34, pp. 10 418–10 430, 2021.
- D. P. Kingma and J. Ba, "Adam: A method for stochastic optimization," in *ICLR*, 2015.
- T. N. Kipf and M. Welling, "Semi-supervised classification with graph convolutional networks," *arXiv preprint arXiv:1609.02907*, 2016.
- W. Kool, H. V. Hoof, and M. Welling, "Attention, learn to solve routing problems!" in *ICLR*, 2019.
- F. Kılıç and M. Gök, "A demand based route generation algorithm for public transit network design," *Computers & Operations Research*, vol. 51, pp. 21–29, 2014. [Online]. Available: <https://www.sciencedirect.com/science/article/pii/S0305054814001300>

- C. Li, L. Bai, W. Liu, L. Yao, and S. T. Waller, "Graph neural network for robust public transit demand prediction," *IEEE Transactions on Intelligent Transportation Systems*, 2020.
- H. Lin and C. Tang, "Analysis and optimization of urban public transport lines based on multiobjective adaptive particle swarm optimization," *IEEE Transactions on Intelligent Transportation Systems*, vol. 23, no. 9, pp. 16 786–16 798, 2022.
- L. Liu, H. J. Miller, and J. Scheff, "The impacts of covid-19 pandemic on public transit demand in the united states," *Plos one*, vol. 15, no. 11, p. e0242476, 2020.
- Y. Ma, J. Li, Z. Cao, W. Song, L. Zhang, Z. Chen, and J. Tang, "Learning to iteratively solve routing problems with dual-aspect collaborative transformer," *Advances in Neural Information Processing Systems*, vol. 34, pp. 11 096–11 107, 2021.
- C. E. Mandl, "Evaluation and optimization of urban public transportation networks," *European Journal of Operational Research*, vol. 5, no. 6, pp. 396–404, 1980.
- A. Mirhoseini, A. Goldie, M. Yazgan, J. W. Jiang, E. Songhori, S. Wang, Y.-J. Lee, E. Johnson, O. Pathak, A. Nazi *et al.*, "A graph placement methodology for fast chip design," *Nature*, vol. 594, no. 7862, pp. 207–212, 2021.
- C. L. Mumford, "Supplementary material for: New heuristic and evolutionary operators for the multi-objective urban transit routing problem, cec 2013," <https://users.cs.cf.ac.uk/C.L.Mumford/Research%20Topics/UTRP/CEC2013Supp.zip>, 2013, accessed: 2023-03-24.
- , "New heuristic and evolutionary operators for the multi-objective urban transit routing problem," in *2013 IEEE congress on evolutionary computation*. IEEE, 2013, pp. 939–946.
- T. N. Mundhenk, M. Landajuela, R. Glatt, C. P. Santiago, D. M. Faissol, and B. K. Petersen, "Symbolic regression via neural-guided genetic programming population seeding," *arXiv preprint arXiv:2111.00053*, 2021.
- M. Nikolić and D. Teodorović, "Transit network design by bee colony optimization," *Expert Systems with Applications*, vol. 40, no. 15, pp. 5945–5955, 2013.
- C. Quak, "Bus line planning," *A passenger-oriented approach of the construction of a global line network and an efficient timetable. Master's thesis, Delft University, Delft, Netherlands*, 2003.
- J.-P. Rodrigue, "Parallel modelling and neural networks: An overview for transportation/land use systems," *Transportation Research Part C: Emerging Technologies*, vol. 5, no. 5, pp. 259–271, 1997.
- [Online]. Available: <https://www.sciencedirect.com/science/article/pii/S0968090X97000144>
- K. Sörensen, "Metaheuristics—the metaphor exposed," *International Transactions in Operational Research*, vol. 22, no. 1, pp. 3–18, 2015.
- K. Sörensen, M. Sevaux, and F. Glover, "A history of metaheuristics," in *Handbook of heuristics*. Springer, 2018, pp. 791–808.
- Statistics Canada, "Census profile, 2021 census of population," 2023, accessed: 2023-10-25. [Online]. Available: <https://www12.statcan.gc.ca/census-recensement/2021/dp-pd/prof/details/page.cfm>
- , "Census dissemination area boundary files," 2021, accessed: 2023-07-01. [Online]. Available: <https://www150.statcan.gc.ca/n1/en/catalogue/92-169-X>
- STL, "Stl gtfs," retrieved 2020. [Online]. Available: <https://transitfeeds.com/p/societe-de-transport-d-e-laval/38/1383528159>
- R. S. Sutton and A. G. Barto, *Reinforcement learning: An introduction*. MIT press, 2018.
- Q. Sykora, M. Ren, and R. Urtasun, "Multi-agent routing value iteration network," in *International Conference on Machine Learning*. PMLR, 2020, pp. 9300–9310.
- R. van Nes, "Multiuser-class urban transit network design," *Transportation Research Record*, vol. 1835, no. 1, pp. 25–33, 2003. [Online]. Available: <https://doi.org/10.3141/1835-04>
- A. Vaswani, N. Shazeer, N. Parmar, J. Uszkoreit, L. Jones, A. N. Gomez, L. Kaiser, and I. Polosukhin, "Attention is all you need," in *Advances in neural information processing systems*, 2017, pp. 5998–6008.
- O. Vinyals, M. Fortunato, and N. Jaitly, "Pointer networks," *arXiv preprint arXiv:1506.03134*, 2015.
- T. Wang, Z. Zhu, J. Zhang, J. Tian, and W. Zhang, "A large-scale traffic signal control algorithm based on multi-layer graph deep reinforcement learning," *Transportation Research Part C: Emerging Technologies*, vol. 162, p. 104582, 2024. [Online]. Available: <https://www.sciencedirect.com/science/article/pii/S0968090X24001037>
- R. J. Williams, "Simple statistical gradient-following algorithms for connectionist reinforcement learning," *Machine learning*, vol. 8, no. 3, pp. 229–256, 1992.
- Y. Wu, W. Song, Z. Cao, J. Zhang, and A. Lim, "Learning improvement heuristics for solving routing problems," *IEEE transactions on neural networks and learning systems*, vol. 33, no. 9, pp. 5057–5069, 2021.
- Y. Xiong and J. B. Schneider, "Transportation network design using a cumulative genetic algorithm and neural network," *Transportation Research Record*, vol. 1364, 1992.

- H. Yan, Z. Cui, X. Chen, and X. Ma, “Distributed multi-agent deep reinforcement learning for multiline dynamic bus timetable optimization,” *IEEE Transactions on Industrial Informatics*, vol. 19, pp. 469–479, 2023.
- J. Yang and Y. Jiang, “Application of modified nsga-ii to the transit network design problem,” *Journal of Advanced Transportation*, vol. 2020, pp. 1–24, 2020.
- R. Ying, R. He, K. Chen, P. Eksombatchai, W. L. Hamilton, and J. Leskovec, “Graph convolutional neural networks for web-scale recommender systems,” *CoRR*, vol. abs/1806.01973, 2018. [Online]. Available: <http://arxiv.org/abs/1806.01973>
- S. Yoo, J. B. Lee, and H. Han, “A reinforcement learning approach for bus network design and frequency setting optimisation,” *Public Transport*, pp. 1–32, 2023.
- L. Zou, J.-m. Xu, and L.-x. Zhu, “Light rail intelligent dispatching system based on reinforcement learning,” in *2006 International Conference on Machine Learning and Cybernetics*, 2006, pp. 2493–2496.
- M. Y. Çodur and A. Tortum, “An artificial intelligent approach to traffic accident estimation: Model development and application,” *Transport*, vol. 24, no. 2, pp. 135–142, 2009.

A Neural Net Architecture

In this section we describe the architecture of the neural net used in our Learned Constructor policy π_θ .

A.1 Input Features

The policy network operates on three types of input: an $n \times 4$ matrix of node feature vectors X , an $n \times n \times 13$ tensor of edge features E , and a global state vector \mathbf{s} .

A node feature x_i is composed of the (x, y) coordinates of the node and its in-degree and out-degree in the street graph.

An edge feature e_{ij} is composed of:

- $s_{ij} = 1$ if $(i, j, \tau_{ij}) \in \mathcal{E}_s$, 0 otherwise
- $c_{ij} = 1$ if \mathcal{R} links i to j , 0 otherwise
- $c_{0ij} = 1$ if j can be reached from i over \mathcal{R} with no transfers, 0 otherwise
- $c_{1ij} = 1$ if one transfer is needed to reach j from i over \mathcal{R} , 0 otherwise
- $c_{2ij} = 1$ if two transfers are needed to reach j from i over \mathcal{R} , 0 otherwise
- self = $(i = j)$, a binary feature indicating whether this edge connects a node to itself
- $\tau_{\mathcal{R}ij}$ if $c_{ij} = 1$, 0 otherwise
- $\tau_{\mathcal{R}ij}$ if $c_{0ij} = 1$, 0 otherwise
- τ_{ij} if $s_{ij} = 1$, 0 otherwise
- D_{ij} , the demand between the nodes
- T_{ij} , the shortest-path driving time between the nodes
- α and $1 - \alpha$, the weights of the two components of the cost function C

The global state vector \mathbf{s} is composed of:

- Average passenger trip time given current route set, $C_p(\mathcal{C}, \mathcal{R})$
- Total route time given current route set, $C_o(\mathcal{C}, \mathcal{R})$
- number of routes planned so far, $|\mathcal{R}|$
- number of routes left to plan, $S - |\mathcal{R}|$
- fraction of node pairs with demand $d_{ij} > 0$ that are not connected by \mathcal{R}
- α and $1 - \alpha$, the weights of the two components of the cost function C

A.2 Policy Network Architecture

The policy π_θ is a neural net with three components: a GNN “backbone”, a halting module NN_{halt} , and an extension module NN_{ext} . The halting and extension modules both operate on the outputs from the GNN. All nonlinearities are ReLU functions. All attention modules are multi-headed with 4 heads. A common embedding dimension of $d_{embed} = 64$ is used; unless otherwise specified, each component of the system outputs vectors of this dimension.

A.2.1 Backbone network

The backbone is a graph attention net composed of five GATv2(Brodry et al., 2021) layers separated by ReLU nonlinearities. The network takes as input the node feature collection X and the edge features E , and the final layer outputs a collection of node embeddings $Y = \{\mathbf{y}_i \forall i \in \mathcal{N}\}$. These node embeddings are used by the two policy heads to compute action probabilities.

A.2.2 Halting module

NN_{halt} is a simple feed-forward MLP. It takes as input the concatenation of the node embeddings of first and last nodes on the current route, the mean of the node embeddings over the graph, \mathbf{s}_t and τ_{r_t} . It outputs a scalar h . We apply the sigmoid function to h get the halting policy:

$$\pi(\text{halt}) = \sigma(h) = \frac{1}{1 + e^{-h}}, \quad \pi(\text{continue}) = 1 - \sigma(h) \quad (10)$$

A.2.3 Extension module

The extension module NN_{ext} is finely tuned to the structure of the cost function. Consider first the case where $\alpha = 1$. We observe that the quality of any candidate route r is then solely a function of the edges (i, j, τ_{rij}) that it adds to the set $\mathcal{E}_{\mathcal{R}}$ of direct-transit-connection edges, where τ_{rij} denotes the time to get from i to j on route r . Therefore, for each path $a \in \text{SP}$ that we consider as an extension of r , a reasonable heuristic is to compute a scalar score o_{ij} for each edge (i, j, τ_{aij}) , and let the path’s score o_a be the sum of the scores of all pairs of nodes that are connected by that path.

Following this intuition, for each node pair (i, j) , we concatenate $[\mathbf{y}_i, \mathbf{y}_j, \mathbf{e}_{ij}, \tau(r + a)_{ij}]$ into a vector and apply an MLP to compute the scalar o_{ij} . For each path $a \in \text{SP}$, we sum these node-pair scores to get path scores: $o_a = \sum_{i,j \in a} o_{ij}$.

If $\alpha < 1$, then the quality of r still depends on the edges it adds to $\mathcal{E}_{\mathcal{R}}$, but also on its time, and whether it is a good

Table 7: Training Hyper-Parameters

Hyper-Parameter	Value
Baseline model learning rate	5×10^{-4}
Baseline model weight decay	0.01
Policy learning rate	0.0016
Policy weight decay	8.4×10^{-4}
Number of training epochs	5
Constraint weight β	5.0
S	10
MIN	2
MAX	12
Adam α	0.001
Adam β_1	0.9
Adam β_2	0.999

choice to extend r by a depends generally on the state \mathcal{S} . So, we concatenate $[o_a, \tau_a, \mathbf{s}_t]$ and apply another MLP to obtain a final score \hat{o}_a for each candidate path. The extension policy is then the softmax of these values:

$$\pi(a) = \frac{e^{\hat{o}_a}}{\sum_{a' \in \mathcal{A}} e^{\hat{o}_{a'}}} \quad (11)$$

A.3 Baseline Network

The baseline function used to compute the learning signal $G_t - b(s_t)$ during training is an MLP with 2 hidden layers of dimension 36. As the return G_t is the same for all t by construction, the baseline need only depend on the details of the problem instance, namely α and \mathcal{C} . The input to $b(s_t)$ is a vector composed of α and several statistics of \mathcal{C} : the average of the node features $\frac{\sum_i \mathbf{x}_i}{n}$, the total demand $\sum_{i,j} D_{ij}$, the means and standard deviations of the elements of D and T , and the cost component weights α and $1 - \alpha$.

A.4 Training Hyper-Parameters

Training was performed using the well-known Adam optimizer Kingma and Ba (2015). Table 7 gives the hyper-parameters used during training. In each epoch of training, we augment the training dataset by applying a set of random transformations. These include rescaling the node positions and by a uniformly-sampled random factor uniformly sampled in the range $[0.4, 1.6]$, rescaling the demand magnitudes by a random factor uniformly sampled in the range $[0.8, 1.2]$, mirroring node positions about the y axis with probability 0.5, and rotating the node positions by a random angle in $[0, 2\pi)$ about their geometric center.

We also randomly sample α separately for each training city in each epoch. Each time α is sampled, it has equal probability of being set to 0.0, set to 1.0, and sampled uniformly in the range $[0, 1]$. This is to encourage the policy to learn both to handle the extreme cases of the passenger perspective and operator perspective, as well as intermediate cases.

This data augmentation lends greater variety to the finite dataset, increasing the performance of the resulting policy on new environments not seen during training.